AMMRC TR 78-17

LASER-PRODUCED STRENGTH DEGRADATION OF PLATES IN TENSION AND TUBES IN TORSION

JIRO ADACHI, ROBERT F. ANASTASI,
and JOHN F. BEATTY
ENGINEERING MECHANICS DIVISION

April 1978

ARMY MATERIALS AND MECHANICS RESEARCH CENTER
Watertown, Massachusetts 02172

UNCLASSIFIED

SECURITY CLASSIFICATION OF THIS PAGE (When Data Entered)

REPORT DOCUMENTATION PAGE

READ INSTRUCTIONS BEFORE COMPLETING FORM

1. REPORT NUMBER (14) AMMRC TR 78-17	2. GOVT ACCESSION NO.
3. RECIPIENT'S CATALOG NUMBER	
4. TITLE (and Subtitle) (6) LASER-PRODUCED STRENGTH DEGRADATION OF PLATES IN TENSION AND TUBES IN TORSION	5. TYPE OF REPORT & PERIOD COVERED (9) Final Report
	6. PERFORMING ORG. REPORT NUMBER
7. AUTHOR(s) Jiro Adachi, Robert F. Anastasi, and John F. Beatty (10)	8. CONTRACT OR GRANT NUMBER(s)
9. PERFORMING ORGANIZATION NAME AND ADDRESS Army Materials and Mechanics Research Center Watertown, Massachusetts 02172 DRXMR-TE	10. PROGRAM ELEMENT, PROJECT, TASK AREA & WORK UNIT NUMBERS D/A Project: 1T162105AH84 AMCMS Code: 612105.H840011 Agency Accession: DA OF4752
11. CONTROLLING OFFICE NAME AND ADDRESS U. S. Army Materiel Development and Readiness Command, Alexandria, Virginia 22333	12. REPORT DATE (11) April 1978
	13. NUMBER OF PAGES 26 (12)
14. MONITORING AGENCY NAME & ADDRESS(if different from Controlling Office)	15. SECURITY CLASS. (of this report) Unclassified
	15a. DECLASSIFICATION/DOWNGRADING SCHEDULE

16. DISTRIBUTION STATEMENT (of this Report)

(35) Approved for public release; distribution unlimited.

17. DISTRIBUTION STATEMENT (of the abstract entered in Block 20, if different from Report)

18. SUPPLEMENTARY NOTES

19. KEY WORDS (Continue on reverse side if necessary and identify by block number)

Laser	Plates	Aluminum alloys
Damage	Tubes	
Failure	Fracture properties	

20. ABSTRACT (Continue on reverse side if necessary and identify by block number)

(SEE REVERSE SIDE)

DD FORM 1 JAN 73 1473 EDITION OF 1 NOV 65 IS OBSOLETE

UNCLASSIFIED

SECURITY CLASSIFICATION OF THIS PAGE (When Data Entered)

Block No. 20

ABSTRACT

Preliminary observations and conclusions regarding laser damage of tension plates and rotating torsion tubes of 7075-T6 aluminum alloy are presented. Good correlations between laser irradiance and physical damage measurements were observed. Load during laser damage has a beneficial effect on fracture strength of tension plates. Torsion tubes are highly susceptible to yielding crippling failure under combined load and narrow laser beam irradiation. Fracture mechanics procedures provide consistent results although scatter of damage and failure results indicate the advisability of using statistical rather than deterministic procedures.

PREFACE

With the exception of minor editorial modifications the contents of this report were presented at the Third DoD Conference on Laser Effects, Vulnerability, and Counter-measures, 19-22 July 1977, at San Diego, California.

The contributions of Robert Fitzpatrick and Thomas Hynes of AMMRC in scheduling and conducting the laser damage tests and in providing a steady flow of technical laser information and the assistance of Miloslav Benicek and Wilbert Foster of AMMRC in obtaining and failure testing the plate specimens are gratefully acknowledged.

CONTENTS

INTRODUCTION

This report presents data obtained from a series of laser damage and residual strength tests performed on tension plates and torsion tubes.

At the present time specimen testing, failure examination and data analysis are only partially completed. However, sufficient information has been developed to permit observations and conclusions which may be helpful to the community in identifying key problem areas and the approach to their solution.

In addition, the data base, in as complete form as possible at this time, is provided for use by other researchers.

BACKGROUND

From the outset this study has aimed at obtaining information from which could be derived the answers (or an indication of the feasibility of deriving answers) to certain questions which are central to the design of structures which survive the damage produced by laser irradiation or other similar effect. First, what types of damage or weakening effects can laser irradiation be expected to produce and what modes of structural failure must be considered probable? Secondly, will it be or is it possible to predict the type and degree of damage or weakening which a given laser can produce in a given structure under given conditions? Finally, can a laser-damaged structure be modeled and analyzed using rational methods to provide accurate predictions of the residual structural performance capabilities of the damaged structure?

It was anticipated that the answer to the first question would develop naturally with increased experience in laser-structure interaction phenomena combined with common engineering judgment. It was necessary only to start. Therefore a selection was made of two basic types of structures which appear commonly.

One structure was the tension or shear plate which is an element of stiffened structures. The other structural element was the torsion tube which is a common element in drive systems. These structural elements differ not only in their structural functioning but also in the survivability philosophy associated with them.[1] The residual structural performance capability of the panel (generally a part of a redundant structure designed for fail-safe behavior) would be based on its residual strength after damage. The torque tube on the other hand usually occurs as a dynamic component whose structural design is based on fatigue life. Therefore its residual structural performance capability would be determined by its residual safe life after damage.

Laser beam quality and power depended on the particular facility used. A key requirement was the capability to simulate the load condition in the structures while damage occurred in order that the behavior of a structure highly

1. RICH, M. J. *Vulnerability Considerations in the Design of Rotary Wing Aircraft Structures* in Proceedings of the Air Force Conference on Fatigue and Fracture of Aircraft Structures and Materials, AFFDL TR 70-144, December 1969, p. 635-651.

loaded during laser damaging could be compared to the behavior of the same structure damaged first and loaded critically afterward. To get preliminary information on the second question of predicting the damaging effects of a given laser it was decided to select visually detectable measures of physical damage and then try to establish a correlation between laser parameter variations and variations in these damage parameters. If the correlation was found to be consistent and at least of a qualitatively predictable nature during these exploratory tests, this would give hope that eventually a quantitatively usable relationship could be developed.

For modeling and analyzing the residual performance of the damaged structures, an approach used earlier for ballistically damaged structures was adopted.[2] This approach combined fracture mechanics procedures with statistical procedures and first defined the damaged structure model necessary for predicting damaged residual strength. Next, a statistical analysis was applied to the scattered values of damage and residual strength associated with ballistically damaged structures to produce probability of survival values. It was expected that laser damage and laser-damaged structural behavior would be characterized similarly by wide scatter which would negate the use of a purely deterministic approach in favor of the statistical approach.

TEST PROCEDURES

Laser Test Facilities

The following laser test facilities were utilized:

a. Tri-Service Laser (TSL), MICOM, Huntsville, AL, April 1976 and December 1976.
b. AFML, LHMEL Laser, WPAFB, OH, June 1976 and November 1976.
c. Ford Aeronutronic, Newport Beach, CA, April 1977.

For tests at TSL MICOM, Ford, and for the first test series at AFML it was necessary to develop special loading jigs for applying tensile loads to the plates and torsional loads plus rotation to the torsion tubes while undergoing laser damage. For the second test series at AFML a Tinius-Olsen 60,000-lb Super L testing machine installed in the test cell was used.

Tension Plate Tests

Test Specimens. The tension plate specimens were 7075-T6 aluminum of flat plate dog-bone configuration 14 inches in overall length, 8-1/2 inches between grips and with a test section 3-1/2 inches wide. Three plate thicknesses, 0.050", 0.095", and 0.250" were used. Values for fracture toughness based on fracture tests of fatigue-cracked center crack specimens performed during the ballistic damage program were 47.0, 41.4, and 36.5 ksi$\sqrt{\text{in.}}$ for nominal 0.050", 0.100", and 0.250" plate thicknesses, respectively. Figure 1 shows the general configuration of the tension plate specimens.

2. RICH, T. P., and ADACHI, J. et al. *Probability Based Fracture Mechanics for Impact Penetration Damage.* International Journal of Fracture, v. 13, no. 4, August 1977, p. 409-430.

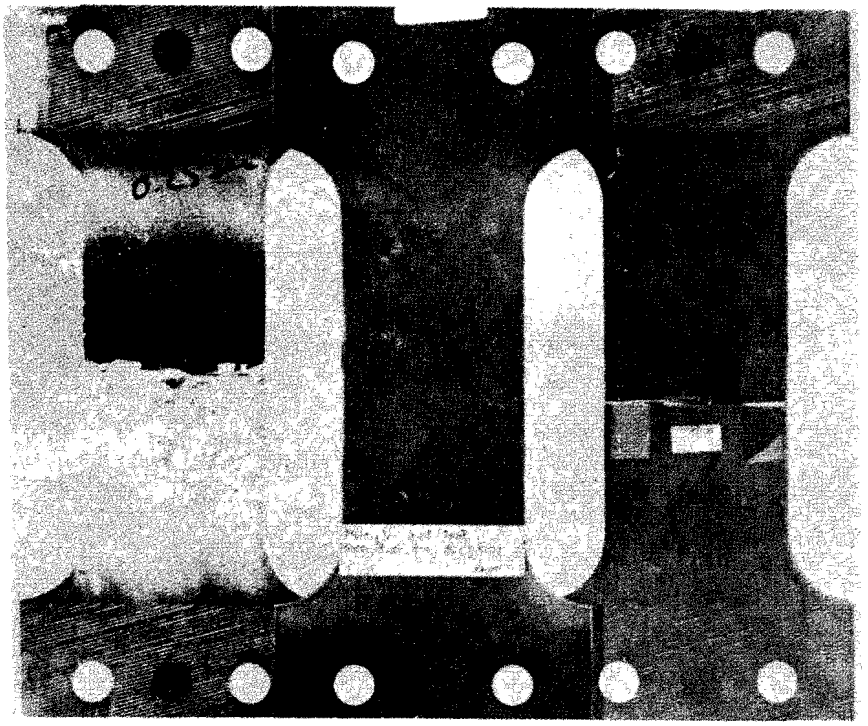

Figure 1. Laser-damaged tension plate specimen.

Test Procedure. Prior to laser irradiation the target area was either polished (POL) using fine emery cloth or was painted (PA) with black spray paint to provide a uniform repeatable surface appearance and laser coupling characteristic. Polished specimens were used primarily in the earlier tests until it was found that excessive laser energy densities were required for appreciable damage. The black paint increased the laser coupling by at least an order of magnitude. One of the problems briefly and unsuccessfully addressed was to determine correlation between beam irradiance, surface finish (POL and PA) and damage. Also during the early tests a series of specimens were damaged without prior surface preparation, either polishing or painting. These are indicated as having natural (NAT) finish.

Tests designated as COLD simulated the damaging of an unloaded structure which was later loaded to failure after having cooled down. Since the initial load was zero for these tests it was necessary only to hold the specimen in the path of the laser. By force of habit the early COLD specimens were set up vertically while being damaged. It was observed that the damage zone was generally symmetric about the vertical axis which was also the gravitational axis. (See Figure 2.) The flow of molten metal occurred vertically downward and it appeared that the degree of damage in the vertical and horizontal directions was quite different and could affect the residual strength. Therefore a series of plates were damaged while oriented horizontally and are so noted in the data records.

As a standard measure of damage the development of a zone of melted metal with pinpoint holes of incipient burnthrough was selected and designated "Condition 2." Partial control of the degree of damage could hopefully be maintained by establishing laser irradiance values for Condition 2 and reducing or increasing laser-on-time to control the damage. Figure 2 shows typical damage levels obtained.

Tests designated as HOT simulated the condition in which a structure is under high load when damaged by laser irradiation. For a true HOT test, failure must occur while the laser beam is irradiating the specimen. A test in which the failure occurs any appreciable time after the laser is off is termed a DELAY test. As a standard procedure a waiting period of 2 minutes was established after which any unfailed specimen was unloaded and removed for COLD testing later.

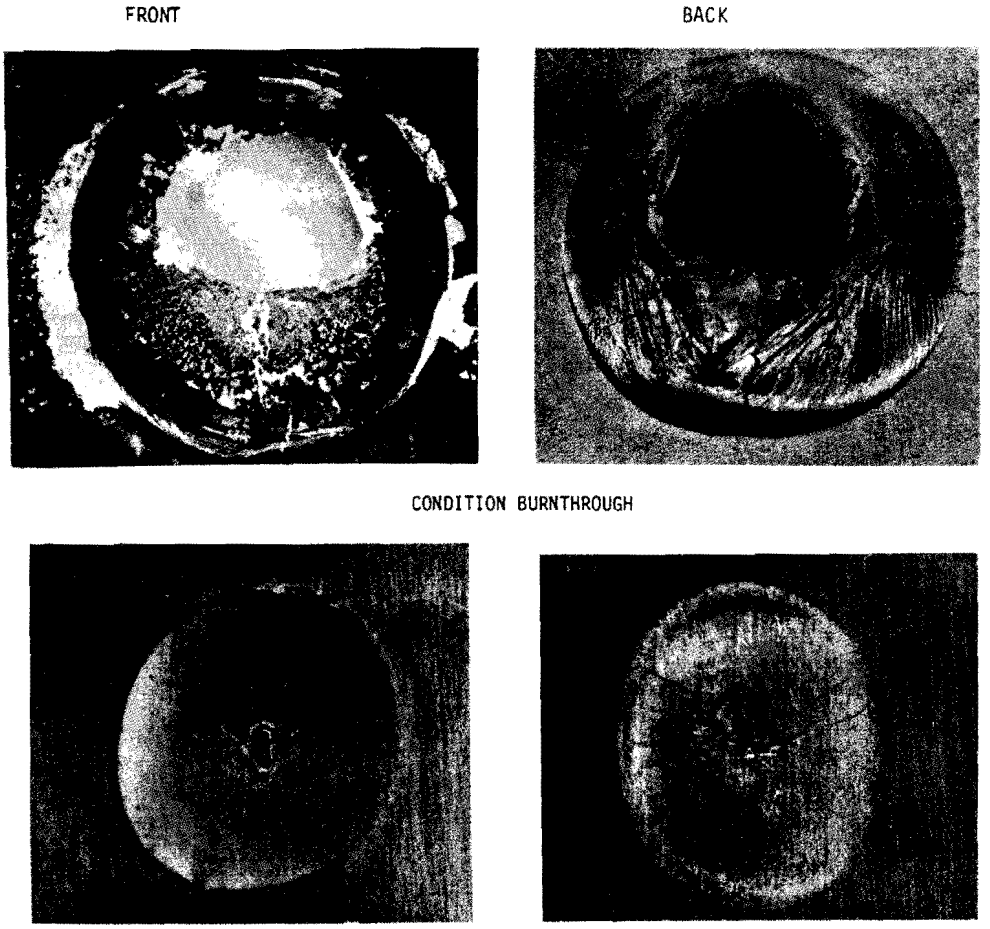

Figure 2. Typical laser damage to plates.

During the second series of tests at AFML in November 1976 it was possible to monitor load on the Tinius-Olsen machine visually from outside the test cell although the controls were not accessible. Records of load value as a function of time were produced as shown in Figure 3. DELAY failures occurred in all the tests shown. However, in other cases with initial load during damage, failure did not occur and the specimens were tested COLD. The fast drop-off load to a minimum and the gradual increase of load is typical of the tension plates. This behavior is attributable to thermal expansion combined with yielding of the heated material which allows the specimen to elongate and causes the load to reduce. The load drop-off would be greater with a stiffer testing machine and smaller with a more flexible machine. The same pattern of behavior would occur in a panel or plate which is part of a redundant structure. Thus the test setup simulates the actual structural environment in which a panel or plate would be operating when damaged.

Selection of Plate Test Parameters and Damage Criteria. In selecting the test conditions for each laser damage test the objective was to cover a range of a selected parameter in order to ascertain if that parameter had a strong effect. The major parameters examined were plate thickness, plate surface condition, initial load, and laser irradiance. In addition, as described above, the effect of orientation of the plate with gravitational axis was briefly tested. Also, the effect of sequence of damage and load as demonstrated by the HOT, DELAY, and COLD test types was examined.

The factors used to measure the effect of these parameters were the damage descriptors (criteria, measures) selected as shown in Figure 4 and the failure strength of the damaged structures. The measurements in Figure 4 are easily made.

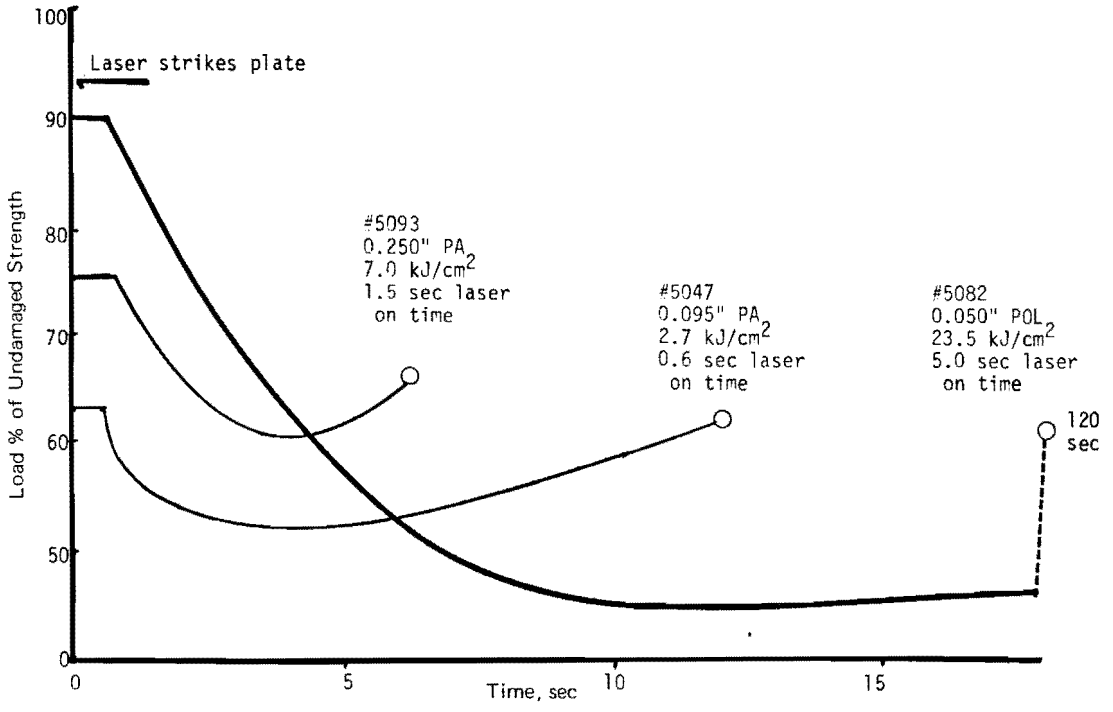

Figure 3. Load versus time during laser heating - 0.050", 0.095", and 0.250" plates.

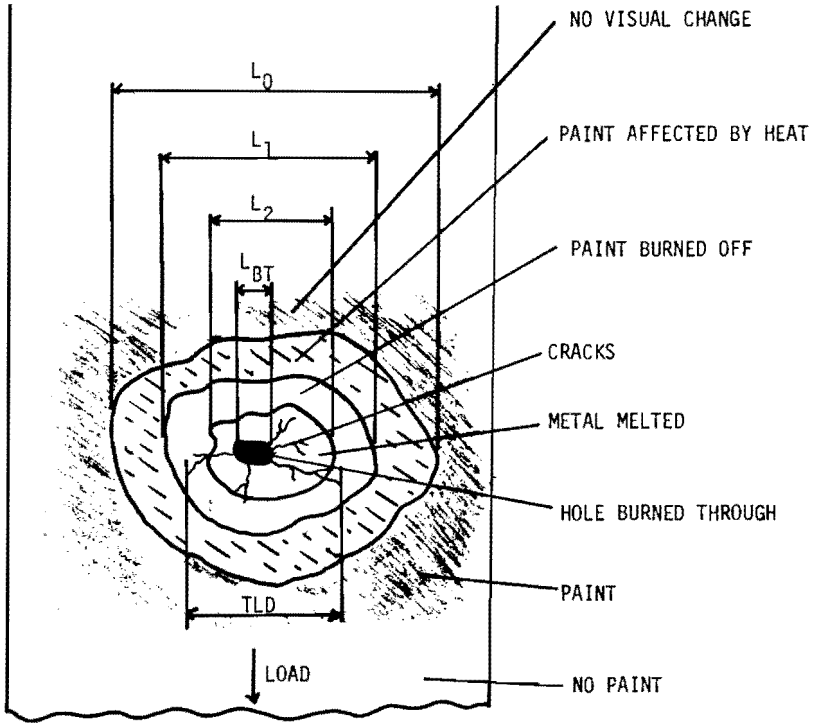

Figure 4. Damage descriptors for tension plates.

L_2, the dimension of the melt zone, L_{BT}, the dimension of the burned-through zone, and TLD, transverse lateral damage, are measures of actual damage. These damage measurements are applicable to all specimens regardless of surface finish. L_0 and L_1, however, are dimensions of the extent of the effect of heat on the paint layer and, although indicative of the severity of the heat input into the plate, have no direct meaning as metal damage measurements.

The rationale for selection of the damage measures is as follows: TLD is a measure of damage commonly used in projectile damage studies[3] and represents the maximum damage dimension measured perpendicular to the direction of principal loading.* This measure of damage has shown to be seriously inadequate under angled crack conditions. However, for preliminary analysis and until the need for more precise damage description is indicated, the TLD measurement will be used. The dimension L_2 is considered important because associated with a metal melt zone is the great probability of shrinkage cracks which develop as cooling takes place. These shrinkage cracks may not be readily detectable and therefore may not be included in TLD. For this study the assumption is made that shrinkage cracks of the dimension L_2 exist. Therefore the larger of L_2 and TLD is used to represent an equivalent crack dimension which is introduced into standard fracture mechanics treatments. All the damage descriptors were selected as indicators of the severity of the laser energy, or rather, the quantity of energy absorbed by the plate. It is hoped and expected that one or a combination of the descriptors will permit

*A damage parameter which takes into account the orientation of the damage pattern with respect to the principal load is available in an earlier paper.[2]

3. BURCH, G. T., and AVERY, J. G. *An Aircraft Structural Combat Damage Model.* v. I, II, III, and Design Handbook, AFFDL TR 50-115, Wright-Patterson Air Force Base, November 1970.

prediction of the amount of laser energy which went into producing the damage. Macroscopic examination of fracture surfaces and macroscopic and microscopic examinations of metallurgical changes in the metal will be used to establish correlation (or the potential for correlation) of the visual criteria with energy absorbed.

Test Data. Test data derived from the plate tests are shown in compact form in Table 1. These tables have been prepared to be self-explanatory and contain all the primary data extracted from the experiments to date. Other data such as detailed crack length and orientation, failure mode and surface data, photomicrographs, and metallurgical analyses are not yet completely available. A sampling of photographs of fracture planes and a micrograph of a similarly irradiated specimen are shown in Figure 5. The melt zone is clearly visible in each photograph. The fracture photographs (a) clearly show the fracture surface developing from the edge of the melt zone. The extent of the initial crack remains to be determined. The micrograph (b) shows the metallurgically heat-affected zone (the narrow light-colored strip adjacent to the melt zone). Discolored areas beyond the heat-affected zones are also heat affected but have not undergone major metallurgical change. Whether or not the change represented by the discoloration is accompanied by significant mechanical property change remains to be determined. Additional information on fracture toughness of the damaged specimens have been derived from the data of Table 1 and are presented in Tables 3 and 4. The discussion of these tables and selected cross plots is left for a later section of the report.

Torsion Tube Tests

Test Specimens. Torsion tube test specimens were 3.0-inch o.d. 7075-T6 aluminum tubes 18" long of three thicknesses: 0.050, 0.095, and 0.250 inch. Figure 6 shows an assortment of tubes after laser damage, some under load. The two tubes on the extreme left were tested but are not covered in this report.

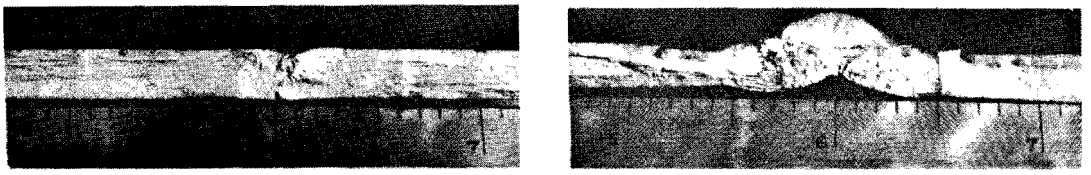

a. Fracture surface.

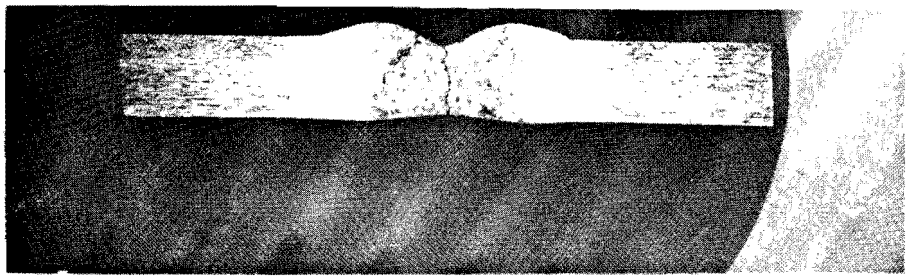

b. Micrograph of 0.250" plate.

Figure 5. Fracture planes and micrograph of irradiated specimens.

Table 1a. TEST DATA FOR 7075-T6 Al TENSION PLATES - 0.050" THICK

Specimen[1]		Laser[2]		Damage[3]					Failure[4]					
Test No.	Surf. Cond.	Time (sec)	Irr (kJ/cm^2)	L_0 (in.)	L_1 (in.)	L_2 (in.)	L_{BT} (in.)	TLD (in.)	Type	Fail Time (sec)	Init. Load (kips[5])	Min. Load (kips)	Last Load (kips)	Fail Load (kips[5])
Tests at AFML, June 1976														
1943	POL	3.0	10.5	-	-	0.3	0	0.05	COLD	-	0	-	-	10.1(71)
1944	POL	3.0	10.5	-	-	0.4	0	0.05	COLD	-	0	-	-	9.5(66)
1945	POL	3.0	10.5	-	-	0.4	0	0.2	COLD	-	0	-	-	9.1(64)
1946	PA	0.22	0.77	1.5	1.0	0.8	0.45	0.65	COLD	-	0	-	-	7.6(53)
1951	POL	2.0	7.0	-	-	0.3	0	0.45	COLD	-	0	-	-	10.9(77)
1952	POL	2.0	7.0	-	-	0.25	0	0.10	COLD	-	0	-	-	10.1(71)
1953	POL	2.0	7.0	-	-	0.4	0	0.30	COLD	-	0	-	-	9.5(66)
1957	POL	2.0	7.0	-	-	0.2	0	0.10	COLD	-	0	-	-	11.3(79)
2066	POL	3.0	10.5	-	-	0.5	0	0.45	COLD	-	9.8(69)	9.2	?	10.1(71)
2067	POL	3.0	10.5	-	-	0.35	0	0.45	COLD	-	11.2(78)	9.8	?	11.0(77)
2068	POL	3.0	10.5	-	-	0.55	0.2	0.6	COLD	-	11.5(81)	9.5	?	10.2(71)
2072	POL	3.0	10.5	-	-	0.6	0	0.45	COLD	-	9.8(69)	8.3	?	9.6(67)
Tests at AFML, Nov 1976														
5000	NAT	3.0	9.9	-	-	0	0	( )	Damage test only. Not strength tested.					
5001	NAT	4.0	13.2	-	-	0	0	( )	"	"	"	"	"	"
5002	NAT	5.0	16.5	-	-	0	0	( )	"	"	"	"	"	"
5003	NAT	9.8	32.2	-	-	0.5	0	0.45	"	"	"	"	"	"
5011	NAT	6.5	29.2	-	-	0.5	0	0.45	"	"	"	"	"	"
5012	NAT	6.5	29.2	-	-	0.8	0.3	( )	COLD	-	0	-	-	8.0(56)
5013	NAT	6.0	27.0	-	-	0.5	0	0.15	COLD	-	0	-	-	8.8(62)
5014	NAT	4.0	18.0	-	-	0.3	0	( )	COLD	-	0	-	-	9.9(70)
5015	NAT	4.0	18.0	-	-	0.7	0.3	0.30	COLD	-	0	-	-	10.5(74)
5016	NAT	4.0	18.0	-	-	0.3	0	( )	COLD	-	0	-	-	10.3(72)
5032	POL	6.0	27.0	-	-	0.7	0	0.7	COLD	-	11.2(79)	5.5	7.5	9.1(64)
5033	POL	6.0	27.0	-	-	0.6	0	0.6	COLD	-	11.7(82)	7.4	9.4	9.8(69)
5034	POL	6.0	27.0	-	-	0.9	0.6	0.7	COLD	-	12.2(86)	4.8	6.6	7.5(53)
5035	POL	6.0	27.0	-	-	0.9	0.6	0.75	COLD	-	12.7(89)	8.1	?	8.1(57)
5036	POL	6.0	27.0	-	-	0.8	0.4	0.63	COLD	-	13.2(93)	7.9	?	7.9(55)
5037	POL	6.0	27.0	-	-	0.9	0.6	0.8	COLD	-	13.7(96)	5.0	?	7.8(55)
5038	POL	6.0	27.0	-	-	0.8	0.6	( )	DELAY	15.0	14.2(100)	5.0	6.0	6.0(42)
5057*	POL	5.0	23.5	-	-	0.6	0.15	0.3	COLD	-	0	-	-	8.0(56)
5058*	POL	5.0	23.5	-	-	0.6	0.15	0.4	COLD	-	0	-	-	8.2(58)
5059*	POL	5.0	23.5	-	-	0.7	0.2	0.45	COLD	-	0	-	-	7.8(55)
5066	POL	6.0	28.2	-	-	0.9	0.4	1.02	COLD	-	11.2(79)	6.4	?	6.9(48)
5075	POL	2.1	10.0	-	-	0.5	0.45	0.55	HOT	2.1	14.2(100)	10.4	10.4	10.4(74)
5076	POL	5.5	26.0	-	-	0.9	0.80	1.0	HOT	5.5	13.7(97)	7.5	7.5	7.5(53)
5077	POL	6.0	28.2	-	-	0.75	0.35	0.85	DELAY	10.8	13.7(97)	6.0	6.0	6.0(42)
5078	POL	5.0	23.5	-	-	0.9	0.6	1.0	DELAY	7.2	13.2(93)	5.8	5.8	5.8(41)
5079	POL	5.0	23.5	-	-	0.85	0.5	1.0	DELAY	9.3	13.2(93)	5.4	5.4	5.4(38)
5080	POL	5.0	23.5	-	-	0.7	0	0.8	COLD	-	12.2(86)	6.6	?	8.3(58)
5082	POL	5.0	23.5	-	-	0.7	0.2	0.8	DELAY	120.0	12.7(90)	6.0	8.7	8.7(61)
5083	POL	5.0	23.5	-	-	0.5	0	( )	COLD	-	0	-	-	8.4(59)
5084	POL	5.0	23.5	-	-	0.5	0	0.34	COLD	-	0	-	-	8.4(59)
5085	POL	5.0	23.5	-	-	0.7	0.2	0.20	COLD	-	0	-	-	9.5(67)

*Specimens horizontal during laser damage.

Notes: 1. Surface conditions: POL - Polished; NAT - Unpolished; PA - Painted Black or Blue.
2. Laser beam spot diameter 0.6". Wavelength 10.6 μm.
3. Specimens vertical during laser damage except as noted. TLD ( ) No visible cracks.
4. Failure: HOT, during lasing; DELAY, ≤ 120 seconds after laser on; COLD, tested later. Load (%), Percent of undamaged strength.
5. Numbers in ( ) are in percentage.
- Not applicable. ? Not recorded.

Table 1b. TEST DATA FOR 7075-T6 Al TENSION PLATES - 0.095" THICK

Specimen[1]		Laser[2]		Damage[3]					Failure[4]					
Test No.	Surf. Cond.	Time (sec)	Irr (kJ/cm²)	L_0 (in.)	L_1 (in.)	L_2 (in.)	L_{BT} (in.)	TLD (in.)	Type	Fail Time (sec)	Init. Load (kips[5])	Min. Load (kips)	Last Load (kips)	Fail Load (kips[5])
Tests at AFML, June 1976														
1947	PA	0.42	1.47	1.1	0.9	0.75	0.4	0.45	COLD	-	0	-	-	11.1(38)
1948	PA	0.30	1.05	0.8	0.6	0.55	0	0.50	COLD	-	0	-	-	14.1(49)
1949	PA	0.30	1.05	0.8	0.6	0.55	0	0.50	COLD	-	0	-	-	13.3(46)
1950	PA	0.30	1.05	0.8	0.6	0.5	0	0.50	COLD	-	0	-	-	14.7(51)
1954	PA	0.20	0.70	?	0.6	0.5	0	0.40	COLD	-	0	-	-	14.4(50)
1955	PA	0.20	0.70	0.8	0.6	0.5	0	0.35	COLD	-	0	-	-	14.7(51)
1956	PA	0.20	0.70	1.0	0.7	0.5	0.1	0.35	COLD	-	0	-	-	15.0(52)
2070	PA	0.30	1.05	1.0	0.6	0.55	0	0.60	COLD	-	18.5(64)	17.4	?	18.5(64)
2071	PA	0.40	1.40	1.1	0.6	0.55	0.25	0.65	COLD	-	18.5(64)	16.2	?	18.1(62)
2073	POL	5.0	17.5	-	-	0.6	0	0.85	COLD	-	18.5(64)	?	?	15.1(52)
2074	POL	5.0	17.5	-	-	0.45	0	0.65	COLD	-	18.5(64)	15.9	?	16.9(58)
Tests at AFML, Nov 1976														
5017	POL	7.0	31.5	-	-	0.65	0	0.65	COLD	-	0	-	-	10.2(35)
5018	POL	7.0	31.5	-	-	0.55	0	0.55	COLD	-	0	-	-	11.2(39)
5019	POL	7.0	31.5	-	-	0.5	0	0.50	COLD	-	0	-	-	11.8(41)
5020	POL	5.5	24.7	-	-	0.55	0	0.5	COLD	-	0	-	-	11.4(39)
5021	POL	4.5	20.2	-	-	0.5	0	0.5	COLD	-	0	-	-	12.0(41)
5022	POL	4.5	20.2	-	-	0.5	0	0.4	COLD	-	0	-	-	12.8(44)
5039	PA	2.0	9.0	1.9	1.2	0.9	0.5	1.1	DELAY	12.2	20.2(70)	11.0	12.0	12.0(41)
5040	PA	1.0	4.5	1.4	0.9	0.7	0.4	0.85	DELAY	8.5	20.2(70)	14.6	15.6	15.6(54)
5041	PA	0.5	2.2	1.1	0.8	0.6	0.4	0.7	DELAY	11.5	20.2(70)	16.0	17.8	17.8(61)
5042	PA	0.25	1.1	0.9	0.6	0.5	0	0.55	DELAY	12.4	20.2(70)	17.6	19.2	19.2(66)
5043	PA	0.25	1.1	0.9	0.6	0.55	0	0.5	COLD	-	12.6(43)	12.0	12.0	17.5(60)
5044	PA	0.25	1.1	0.9	0.6	0.55	0	0.55	COLD	-	16.4(57)	15.6	16.4	18.4(63)
5045	PA	0.25	1.1	0.9	0.6	0.6	0	0.5	COLD	-	18.3(63)	16.8	18.3	19.0(65)
5046	PA	1.0	4.5	1.5	1.0	0.8	0.5	0.9	DELAY	12.4	18.3(63)	14.4	15.6	15.6(54)
5047	PA	0.6	2.7	1.2	0.9	0.6	0.4	0.7	DELAY	12.0	18.3(63)	15.2	18.0	18.0(62)
5067	PA	0.25	1.2	0.9	0.6	0.5	0	0.55	COLD	-	20.2(70)	17.6	19.2	18.9(65)
5068	PA	0.25	1.2	0.7	0.6	0.5	0.4	0.4	HOT	0.3	25.0(86)	25.0	25.0	25.0(86)
5069	PA	0.25	1.2	0.9	0.6	0.5	0	0.5	DELAY	60.0	22.5(78)	18.0	19.5	19.5(67)
5070	PA	0.25	1.2	1.0	0.65	0.55	0	0.65	DELAY	42.0	23.5(81)	17.5	19.0	19.0(66)
5071	PA	0.25	1.2	0.9	0.6	0.55	0	0.6	DELAY	35.0	23.5(81)	18.0	19.5	19.5(67)
5072	PA	0.25	1.2	0.9	0.6	0.55	0	0.45	COLD	-	0	-	-	15.6(54)
5073	PA	0.25	1.2	0.9	0.6	0.55	0	0.5	COLD	-	0	-	-	15.0(52)
5074	PA	0.25	1.2	0.9	0.6	0.5	0	0.5	COLD	-	0	-	-	14.1(49)

Notes: 1. Surface conditions: POL - Polished; NAT - Unpolished; PA - Painted Black or Blue.
2. Laser beam spot diameter 0.6". Wavelength 10.6 μm.
3. Specimens vertical during laser damage except as noted.
4. Failure: HOT, during lasing; DELAY, ≤ 120 seconds after laser on; COLD, tested later. Load (%), Percent of undamaged strength.
5. Numbers in ( ) are in percentage.
- Not applicable. ? Not recorded.

Table 1c. TEST DATA FOR 7075-T6 Al TENSION PLATES - 0.250" THICK

Specimen[1]		Laser[2]		Damage[3]					Failure[4]					
Test No.	Surf. Cond.	Time (sec)	Irr (kJ/cm²)	L_0 (in.)	L_1 (in.)	L_2 (in.)	L_{BT} (in.)	TLD (in.)	Type	Fail Time (sec)	Init. Load (kips[5])	Min. Load (kips)	Last Load (kips)	Fail Load (kips[5])
Tests at AFML, 29 Nov 1976														
5026	PA	0.5	2.25	0.7	0.6	0.55	0	( )	COLD	-	0	-	-	59.0(78)
5027	PA	0.7	3.15	0.8	0.6	0.55	0	( )	COLD	-	0	-	-	61.0(81)
5028	PA	1.0	4.50	0.9	0.6	0.55	0	0.6	COLD	-	0	-	-	45.3(60)
5029	PA	5.06	22.8	2.5	1.6	1.1	0.3	0.95	COLD	-	0	-	-	25.2(35)
5030	PA	2.5	11.2	1.6	0.9	0.7	0	( )	COLD	-	0	-	-	40.5(54)
5090	PA	2.5	11.7	1.4	0.9	0.8	0.7	1.0	HOT	2.5	56.5(75)	49.0	49.0	49.0(65)
5091	PA	2.0	9.4	1.4	0.8	0.6	0.4	0.7	DELAY	3.7	56.5(75)	45.6	45.6	45.6(61)
5092	PA	1.0	4.7	1.0	0.7	0.55	0	0.7	COLD	-	56.5(75)	55.0	56.5	57.6(76)
5093	PA	1.5	7.0	1.3	0.8	0.6	0.3	0.8	DELAY	6.2	56.5(75)	45.0	50.0	50.0(66)
5094	PA	1.25	5.9	1.2	0.8	0.6	0.2	0.8	DELAY	6.0	56.5(75)	50.5	50.5	50.5(67)
5095	PA	1.5	7.0	1.2	0.8	0.6	0.1	0.5	COLD	-	50.0(67)	46.0	50.0	52.7(70)
5096	PA	2.0	9.4	1.5	0.9	0.7	0.1	0.8	COLD	-	50.0(67)	43.0	50.0	53.0(70)
5097	PA	3.0	14.1	1.8	1.1	0.8	0.2	1.2	DELAY	47.0	50.0(67)	36.5	46.6	46.6(61)
5098	PA	2.0	9.4	1.2	0.8	0.65	0	( )	COLD	-	0	-	-	35.4(47)
5099	PA	2.0	9.4	1.4	0.9	0.65	0.1	( )	COLD	-	0	-	-	30.8(41)
5100	PA	2.0	9.4	1.4	0.9	0.75	0.1	0.6	COLD	-	0	-	-	32.4(43)

Notes: 1. Surface conditions: POL - Polished; NAT - Unpolished; PA - Painted Black or Blue.
2. Laser beam spot diameter 0.6". Wavelength 10.6 μm.
3. Specimens vertical during laser damage except as noted. TLD ( ) No visible cracks. Damage of front face only. Back face damage is usually less severe.
4. Failure: HOT, during lasing; DELAY, ≤ 120 seconds after laser on; COLD, tested later. Load (%), Percent of undamaged strength.
5. Numbers in ( ) are in percentage.
- Not applicable. ? Not recorded

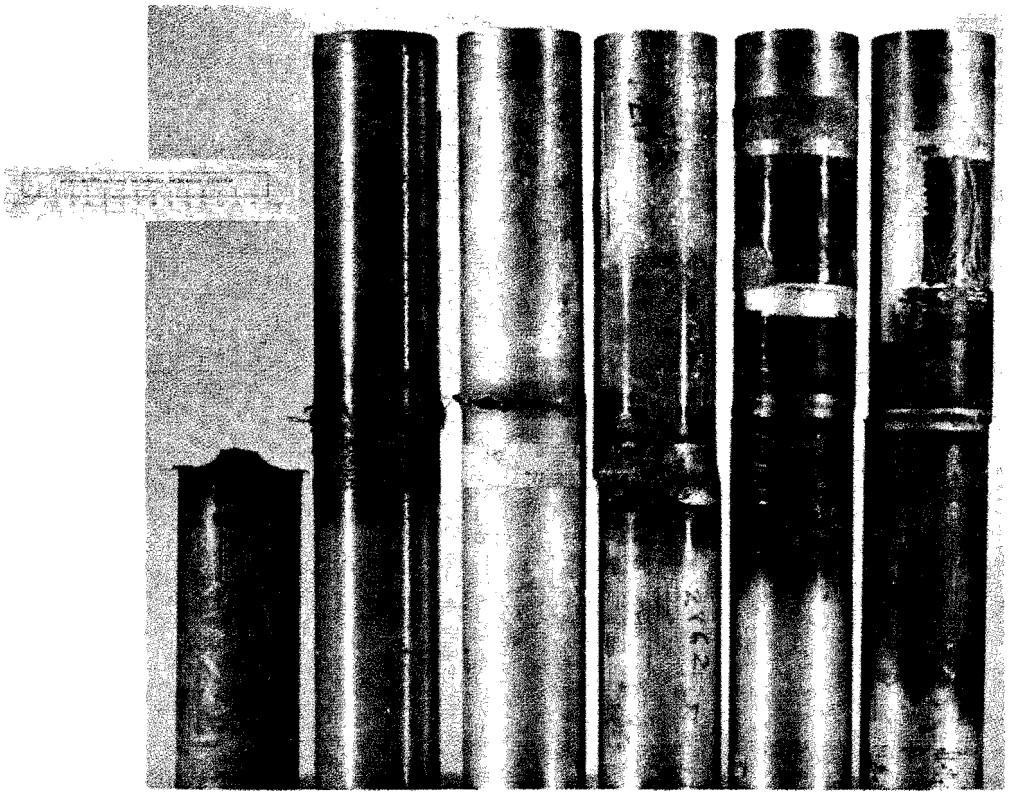

Figure 6. Typical torsion tubes following laser damage testing.

Test Procedure. As in the testing of tension plates it was desired to damage the tubes by laser irradiation in the unloaded and loaded conditions to determine whether failure during damage, a HOT test, occurred at a lower or higher load than failure in a COLD test (load after laser damage and cooling). A simple test system was devised which applied a fixed torsional load to a tube by utilizing an internal rod to provide the necessary torsional reaction. Wedge ring clamps were used to clamp the tube to the rod while the rod was pretorqued by a torque wrench. Release of the torque wrench introduced torque into the tube. The entire assembly was then placed in a wood-turning lathe located in the path of the damaging laser beam and rotated at the desired speed. A speed of 1350 rpm was arbitrarily selected. Figure 7 shows a close-up of a damaged tube clamped to the square reaction rod. Figure 8 shows the assembled torque tube mounted in the wood-turning lathe. The open-ended plexiglass structure through which the tube passes is a guard to prevent molten metal spray from reaching the laser mirror or lens. The rectangular hole in the spray guard is the aperture for the laser beam. (Immediately to the right of the spray guard can be seen a Moiré interference fringe pattern sensitive to the torque load on the tube. This was part of an experimental system which used a synchronized strobe-light camera system to photograph change in the fringe pattern (and torque) as the tube was laser damaged.) The torquing system requires further improvement to increase the magnitudes of the pretorque that can be applied to the tube. Also, a slip-ring system for taking off thermocouple and strain readings must be added. A further refinement would be to utilize a loading system which would maintain a constant load level with a superimposed periodic load variation to simulate the fatiguing loads experienced by torque transmitting components.

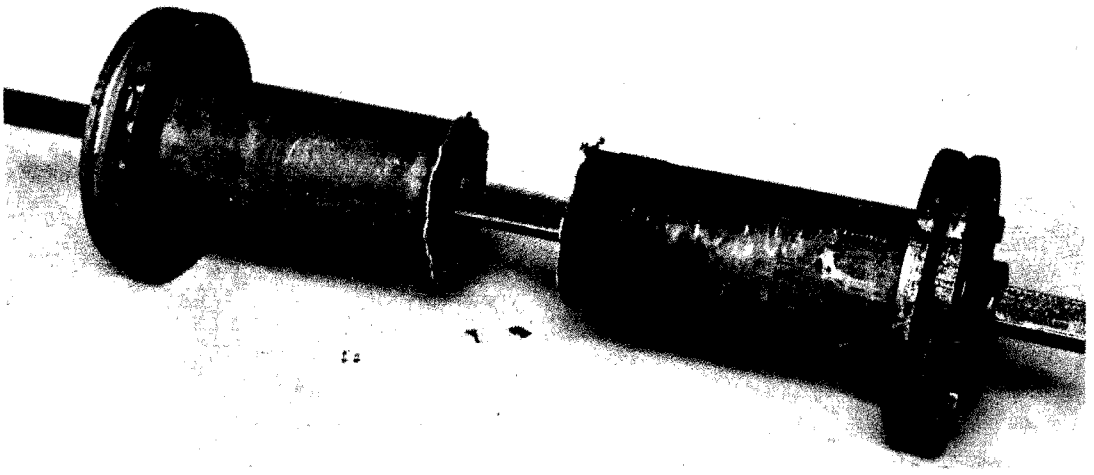

Figure 7. Pretorque system with laser damaged tube.

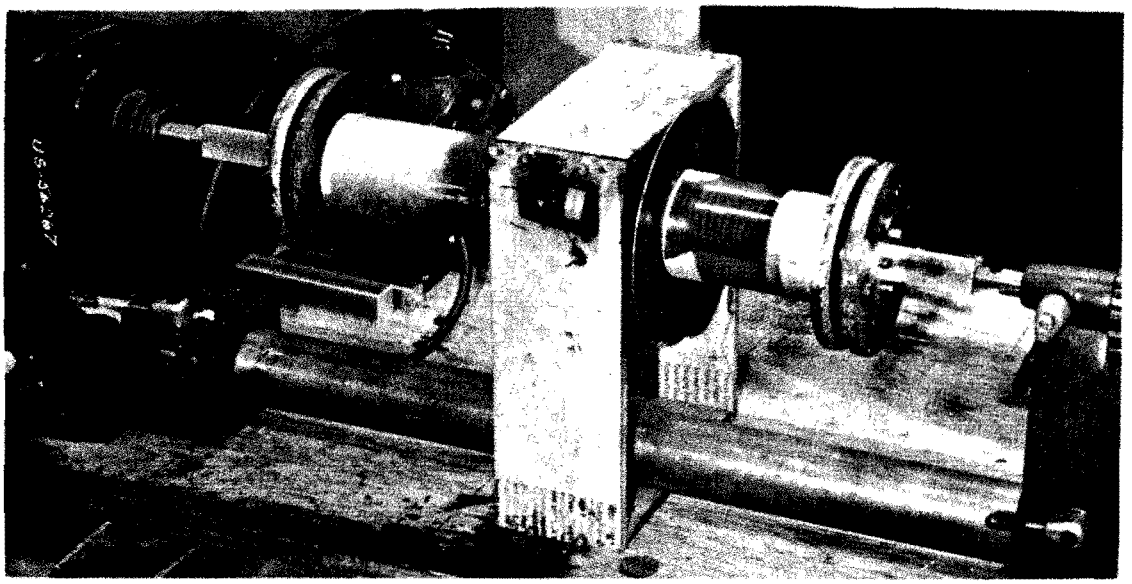

Figure 8. Tube rotating system.

Prior to exposing the tube to laser damage the surface of the tube was prepared either by polishing with emery cloth or by spray painting with black or dark blue paint, the purpose being to maintain uniform coupling between the surface and the laser beam.

Test Data. Test data derived from the torsion tube tests are shown in Table 2. The data are not complete since COLD tests on the remaining unfailed specimens have not been performed nor have micrographic studies been completed. In addition, peak irradiance values (Irr Peak) for the TSL MICOM test series were not obtained and cannot be simply computed as was done for the AFML and Ford test series.

Table 2a. TEST DATA FOR 7075-T6 ROTATING TUBES - 0.050" THICK x 3.0" OD

Specimen[1]		Laser Beam[2]				Damage[3]					Failure[4]			
Test No.	Surf. Cond.	Time (sec)	Irr Avg. (kJ/cm²)	Irr Peak (kJ/cm²)	Beam Size (in.)	W_0 (in.)	W_1 (in.)	W_2 (in.)	W_{BT} (in.)	L_D %	Init Load (ft-lb[5])	Type	Fail Time (sec)	Fail Load (ft-lb[5])
Tested at TSL[6] MICOM, May 1976														
2071	POL	2.2	4.25	?		-	-	?	0	74	260(10)	HOT	?	260(10)
2072	POL	2.2	4.05	?		-	-	?	0	100	260(10)	HOT	?	260(10)
2084	POL	2.15	4.4	?		-	-	?	0	68	260(10)	HOT	?	260(10)
2120	POL	2.0	4.0	?		0	0	0	0	0	0	(To be COLD tested)		
Tested at AFML,[7] Nov 1976														
5115	PA	3.5	16.5	1.03	0.6	?	0.8	0.45	0.12	100	0	HOT	?	0
5123	PA	2.0	9.4	0.59	0.6	1.6	0.6	0.2	0	0	0	(To be COLD tested)		
5124	PA	2.5	11.75	0.74	0.6	1.7	0.7	0.25	0	55	0	"	"	"
5125*	PA	2.5	11.75	0.74	0.6	1.6	0.7	0.2	0	58	0	"	"	"
Tested at Ford Aeronutronic,[8] April 1976														
050-1a	PA	2.8	8.7	0.74	0.6	(Void Beam Blocked)				-	(Damage test, No strength test)			
b	PA	3.4	10.5	0.89	0.6	(Tube burned off)			0.6	-	"	"	"	"
c	PA	3.1	9.7	0.82	0.6	"	"	"	0.6	-	"	"	"	"
d	PA	2.8	8.8	0.75	0.6	"	"	"	0.6	-	"	"	"	"
e	PA	1.9	5.7	0.48	0.6	?	0.6	0.3	0	53	"	"	"	"
f	PA	2.1	6.4	0.54	0.6	?	0.6	0.35	0	79	"	"	"	"
050-2a	PA	1.0	3.1	0.26	0.6	0.8	0.6	0	0	0	474(18)	None	-	-
b	PA	1.4	4.2	0.36	0.6	1.2	0.6	0.15	0	12	474(18)	HOT	?	474(18)
050-3	PA	1.4	4.3	0.36	0.6	1.2	0.7	0.25	0	0	0	(To be COLD tested)		
050-4	PA	1.4	4.3	0.36	0.6	1.1	0.6	0.3	0	0	0	"	"	"
050-5	PA	1.4	4.3	0.36	0.6	1.2	0.55	0.2	0	86	474(18)	HOT	?	474(18)
050-6	PA	1.4	4.3	0.36	0.6	1.2	0.55	0.1	0	29	474(18)	HOT	?	474(18)
050-7	PA	1.4	4.4	0.37	0.6	1.2	0.55	0.2	0	74	237(9)	HOT	?	237(18)
050-8	PA	1.2	3.8	0.32	0.6	1.0	0.55	0.25	0	0	474(18)	HOT	?	474(18)
050-9	PA	1.2	3.7	0.31	0.6	1.1	0.55	0.25	0	0	0	(To be COLD tested)		
050-10	PA	1.2	3.7	0.31	0.6	1.0	0.55	0.25	0	0	474(18)	HOT	?	474(18)

*Crack 1.7" lengthwise of tube.

Tests:
1. Surface conditions: POL - Polished; NAT - Unpolished; PA - Painted Black or Blue. Rotation, 1350 rpm unless otherwise noted.
2. Average Irr values are laser beam values. Peak Irr values are as received by specimen. Beam size measured lengthwise of tube.
3. W measured lengthwise of tube. L_D, % of the tube circumference cracked or separated.
4. HOT, during lasing; COLD, tested after laser irradiation. Init. Load (%), Torque (% of undamaged) at start of lasing.
5. Numbers in ( ) are in percentage.
6. Wavelength 10.6 μm. Peak = 3x average power density.
7. Wavelength 10.6 μm. Uniform power density. Peak = average. Beam on specimen 0.6" d.
8. Wavelength 10.6 μm. Uniform power density. Peak = average. Beam on specimen 0.6" width x 0.8" along tube circumference.

\- Not applicable. ? Unknown.

Table 2b. TEST DATA FOR 7075-T6 ROTATING TUBES - 0.095" THICK x 3.0" OD

Specimen[1]		Laser Beam[2]				Damage[3]					Failure[4]			
Test No.	Surf. Cond.	Time (sec)	Irr Avg. (kJ/cm²)	Irr Peak (kJ/cm²)	Beam Size (in.)	W_0 (in.)	W_1 (in.)	W_2 (in.)	W_{BT} (in.)	L_D %	Init. Load (ft-lb[5])	Type	Fail Time (sec)	Fail Load (ft-lb[5])
Tested at TSL[6] MICOM, May 1976														
2086	POL	2.2	4.3	?		-	-	(No visible damage)			-	-	-	-
Tested at AFML,[7] Nov 1976														
5116*	PA	2.0	9.8	0.62	0.6	?	?	(No visible damage)			0	-	-	-
5119*	PA	4.0	19.6	1.25	0.6	?	?	"	"	"	0	-	-	-
5120*	PA	6.0	29.3	1.87	0.6	?	0.55	"	"	"	0	-	-	-
5121*	PA	8.0	39.1	2.49	0.6	?	0.55	"	"	"	0	-	-	-
5122*	PA	10.0	48.9	3.11	0.6	1.5	0.6	0.2	0	94	0	(To be COLD tested)		
5127	PA	10.0	48.9	3.11	0.6	1.5	0.55	0.2	0	85	180(3.6)	HOT	?	180(3.6)
Tested at TSL[6] MICOM, May 1976														
2453	PA	1.07	4.4	?		2.2	0.9	0.6	0	89	0	-	-	-
2454	PA	1.07	4.2	?		1.8	1.1	0.25	0	0	0	-	-	-
2455*	PA	1.05	5.8	?		?	?	(No visible damage)			180(3.6)	(To be COLD tested)		
2456*	PA	1.55	8.5	?		2.4	1.3	0.9	0	100	180(3.6)	HOT	?	180(3.6)
2460	FRP†	1.60	7.2	?				(Metal untouched. FRP surface charred.)						
Tested at Ford Aeronutronic,[8] April 1976														
0.100-1a	PA	3.1	35.1	1.7	0.30	?	0.35	0	0	0	0	-	-	-
1b	PA	4.1	46.5	2.2	0.30	?	0.35	0	0	0	0	-	-	-
1c	PA	5.8	65.0	3.1	0.30	?	0.35	0	0	0	0	-	-	-
1d	PA	5.5	93.7	3.4	0.26	?	0.3	0.2	0	0	0	-	-	-
1e	PA	5.1	113.0	3.6	0.22	?	0.25	0	0	0	0	(To be COLD tested)		
2	PA	5.1	113.0	3.6	0.22	1.8	0.25	0	0	0	522(11)	"	"	"

*Same TUBE repainted and used.
†FRP - S-Glass/Epoxy 90° protective wrapping 0.025± inch thick.

Notes:
1. Surface conditions: POL - Polished; NAT - Unpolished; PA - Painted Black or Blue. Rotation, 1350 rpm unless otherwise noted.
2. Average Irr values are laser beam values. Peak Irr values are as received by specimen. Beam size measured lengthwise of tube.
3. W measured lengthwise of tube. L_D, % of the tube circumference cracked or separated.
4. HOT, during lasing; COLD, tested after laser irradiation. Init. Load (%), Torque (% of undamaged) at start of lasing.
5. Numbers in ( ) are in percentage.
6. Wavelength 10.6 μm. Peak = 3x average power denstiy.
7. Wavelength 10.6 μm. Uniform power density. Peak = average. Beam on specimen 0.6" d.
8. Wavelength 10.6 μm. Uniform power density. Peak = average. Beam on specimen, 0.6" width x 0.8" along tube circumference.

\- Not applicable. ? Unknown.

Table 2c. TEST DATA FOR 7075-T6 ROTATING TUBES - 0.250" THICK x 3.0" OD

Specimen[1]		Laser Beam[2]				Damage[3]					Failure[4]			
Test No.	Surf. Cond.	Time (sec)	Irr Avg. (kJ/cm²)	Irr Peak (kJ/cm²)	Beam Size (in.)	W_0 (in.)	W_1 (in.)	W_2 (in.)	W_{BT} (in.)	L_D %	Init. Load (ft-lb⁵)	Type	Fail Time (sec)	Fail Load (ft-lb⁵)
Tested at TSL[6] MICOM, May 1976														
2083	NAT	2.16	4.3	?				(No visible damage)			235(2.2)	None	-	-
2088	NAT	4.2	8.2	?				"	"	"	0	-	-	-
2102	NAT	2.1	10.5	?				"	"	"	0	-	-	-
2115	NAT	4.0	20.5	?				"	"	"	0	-	-	-
Tested at AFML,[7] Nov 1976														
5117*	PA	5.0	23.5	1.5	0.6			(No visible damage)			0	-	-	-
5118*†	PA	7.0	32.9	2.1	0.6	?	1.8	1.2	0.3	7	0	(To be COLD tested)		
Tested at TSL[6] MICOM, Dec 1976														
2461	PA	3.28	14.8	?		2.5	1.3	0.4	0	34	0	(To be COLD tested)		
2462	PA	3.25	16.6	?		2.5	1.4	0.7	0	100	588(5.4)	HOT	?	588(5.4)

*Same specimen.
†Tube not rotating. Damage dimensions shown are L_0, L_1, L_2, L_{BT} (Figure 4), and L_D.

Notes: 1. Surface conditions: POL - Polished; NAT - Unpolished; PA - Painted Black or Blue. Rotation, 1350 rpm unless otherwise noted.
2. Average Irr values are laser beam values. Peak Irr values are as received by specimen. Beam size measured lengthwise of tube.
3. W measured lengthwise of tube. L_D, % of the tube circumference cracked or separated.
4. HOT, during lasing; COLD, tested after laser irradiation. Init. Load (%), Torque (% of undamaged) at start of lasing.
5. Numbers in ( ) are in percentage.
6. Wavelength 10.6 μm. Peak = 3x average power density.
7. Wavelength 10.6 μm. Uniform power density. Peak = average. Beam on specimen 0.6" d.
- Not applicable. ? Unknown

Irr Peak values are the values of the irradiance received by the rotating tube from the laser beam. In the case of a laser beam irradiating a fixed target, energy density distributions can be calibrated by test burns of plexiglass disks in which the depth of burn is a measure of the density and the beam depth profile gives the energy density distributions. To determine the energy density profile along a rotating tube a similar burn pattern should be taken on a rotating plexiglass tube. Otherwise, except in the case of a beam whose density profile is flat, the energy density on a tubular specimen cannot be determined without a great deal of difficulty. In the case of laser beam with a flat-topped density profile irradiating a rotating tube the irradiance on the tube is equal to the laser beam irradiance multiplied by the ratio of the beam dimension along the tube circumference to the tube circumference itself. The values shown for the AFML and Ford tests were so determined. However, in the case of a nonuniform beam which has a nonflat and possibly a very complicated profile in the direction along the tube circumference, it would be necessary at the very least to integrate the beam profile along the tube circumference for small incremental steps parallel to the tube axis. The lack of this piece of data precludes meaningful comparison of the TSL MICOM data to that from other test series.

The damage descriptors or measures used for the torsion tube damage are shown in Figure 9. These are similar in nature to the tension plate damage descriptors and were devised for the same purpose. Further discussion of the data is left for later portions of this report.

ANALYSIS OF TEST RESULTS

Analysis of Test Results on Plates

Physical Damage Effects of Laser Irradiation. In order to be able to determine the laser energy level that produced a given amount of damage or, conversely, to predict the degree of damage for a given energy input it is necessary to select a damage measure that has a one-to-one relationship to laser energy. Figure 10 is

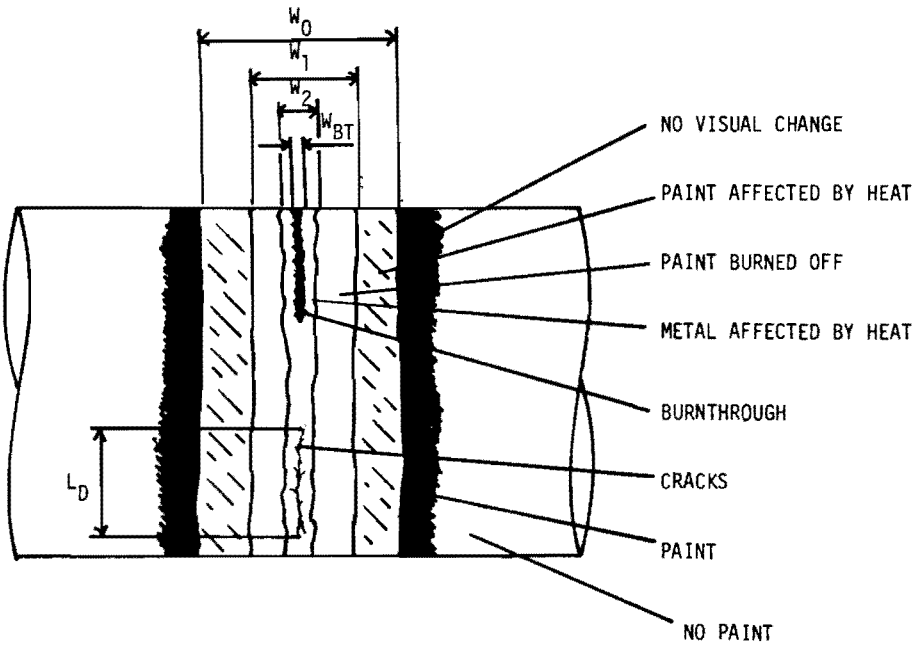

Figure 9. Damage descriptors for torsion tubes.

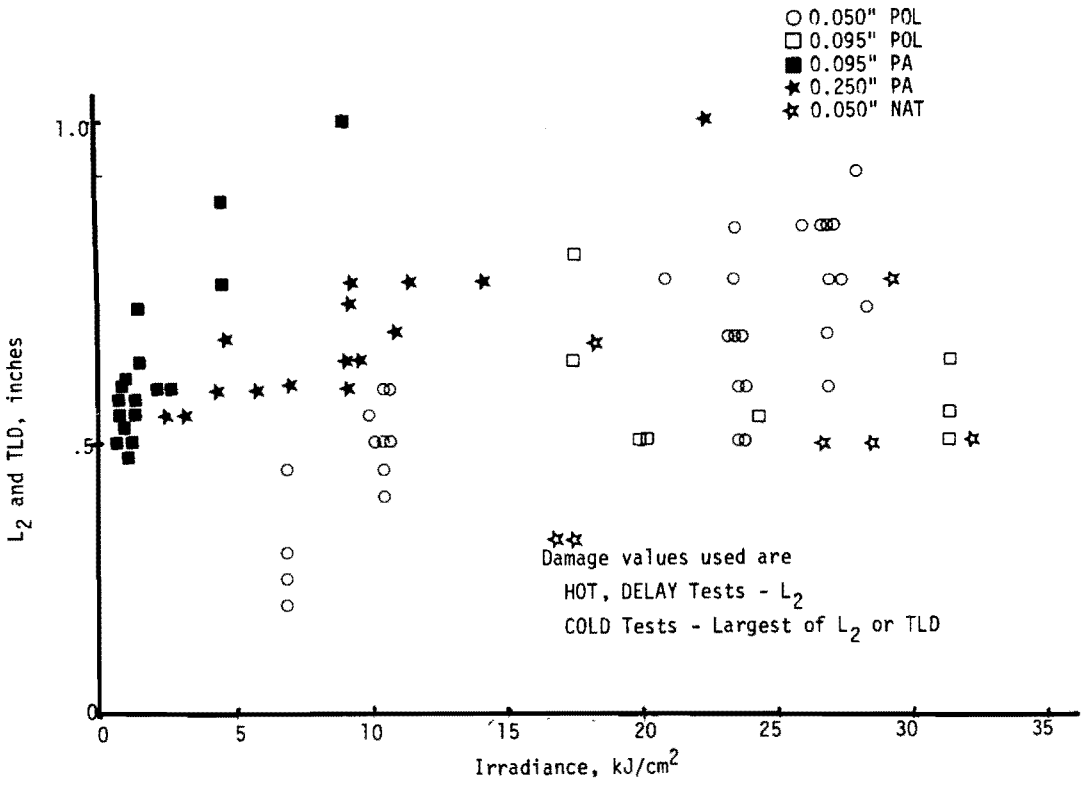

Figure 10. Damage versus irradiance for tension plates.

a plot of damage measures L_2 or TLD obtained for various energy irradiance values. L_2 was used as the damage measure for HOT and DELAY tests since only post-failure examination for cracks was possible and it was observed that cracks were produced and extended before and during the failure process. For the COLD tests inspection for TLD before test to failure was possible and therefore the larger of L_2 or TLD was used. The plot shows definite qualitative relationship between L_2 or TLD and laser irradiance with the exception of the polished 0.095"-thick (0.095 POL) data which are erratic.

The scatter band of the polished 0.050"-thick (0.050 POL) data is quite broad in the higher irradiance levels which is where the polished 0.095" data is erratic. Since the data is not separated in terms of different initial load values it is possible that initial load differences are the cause of the scatter. It is further possible that the large scatter is the result of variations in the absorbed energy which is more sensitive to variation in surface conditions at higher reflectivity.

However, the well-defined relationships demonstrated by the data for painted specimens are a good indication that suitably reliable quantitative relationships between the damage descriptors L_2 and TLD and laser irradiance can be found for painted or more absorptive surface conditions. Similarly reliable relationships for polished surfaces are probably unlikely to be found.

Strength Reducing Effects of Laser Irradiation. The above-mentioned effects of irradiation on damage measure should be reflected in a reduction of mechanical strength unless other physical changes, such as in material properties, are significant. Figure 11 shows the relationship of irradiance to the failure strength in COLD tests with no initial load on the specimen. The expected effect indicated by Figure 10 is evident in this figure. The scatter band is much narrower but the number of data points is much smaller. However, the indication here is that no other physical changes have occurred which would counterbalance the damage-increasing tendency of increased irradiance. In this figure also is shown the effect of the relative orientation of the direction of gravity to the direction of load. Six 0.050" POL tests at 23.5 kJ/cm^2 irradiance were damaged under no initial load with three oriented vertically during damage and three oriented horizontally during damage. These data show that there is some effect although of the same order of magnitude as the scatter associated with the 0.050" POL data. Further examination of this effect is necessary. Figure 12 shows effect of irradiance on failure strength for different levels of initial load. The strength-reducing effect of higher irradiance is consistently evident here also.

Effect of Initial Load Level on Failure Strength. Figure 13 shows the effect of initial load during laser damage of polished 0.050" plates for different laser irradiance levels. There is a large gap in the data between 0% and 65% initial load which precludes any definite statement relating zero initial load data to higher initial load data. However, for relatively lower levels of irradiance of 10.0 to 10.5 kJ/cm^2 (for polished specimens), change in initial load between 65% and 100% of undamaged strength has little effect with possibly a slight increase of the failure strength. However, for the relatively higher irradiance, increase in initial load at the higher percentages of undamaged strength causes a sharp downward trend in failure strength. Examination of the Table 1 load drop-off data

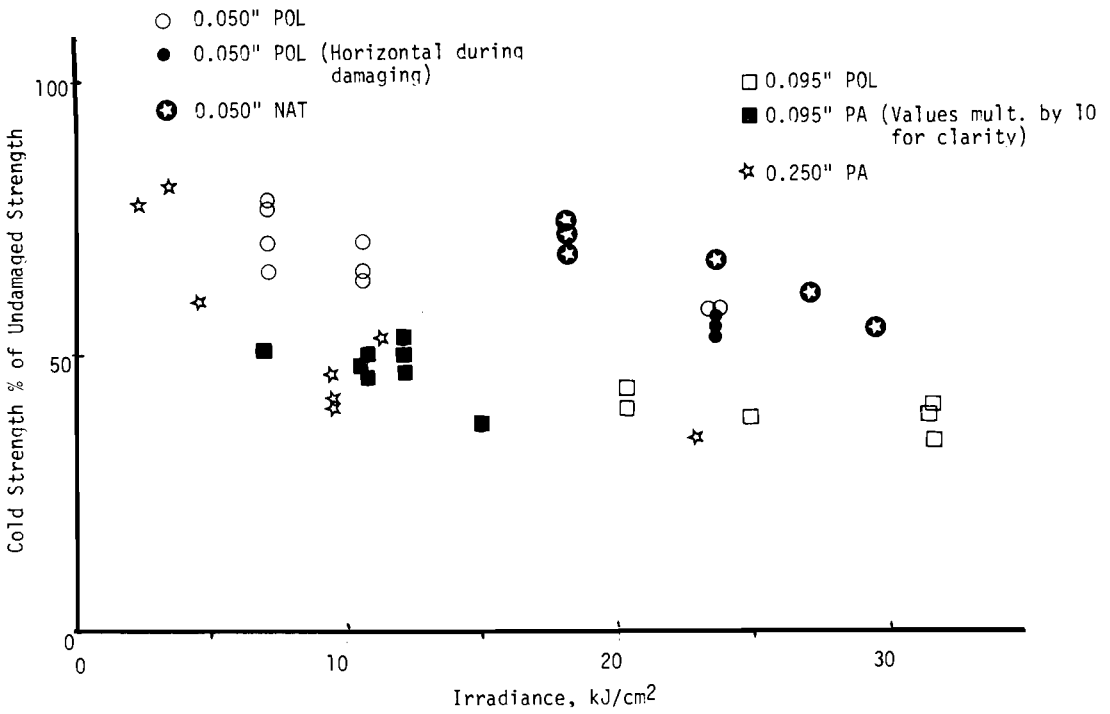

Figure 11. Cold strength versus irradiance 0.050", 0.095", and 0.250" plates, initial load = 0.

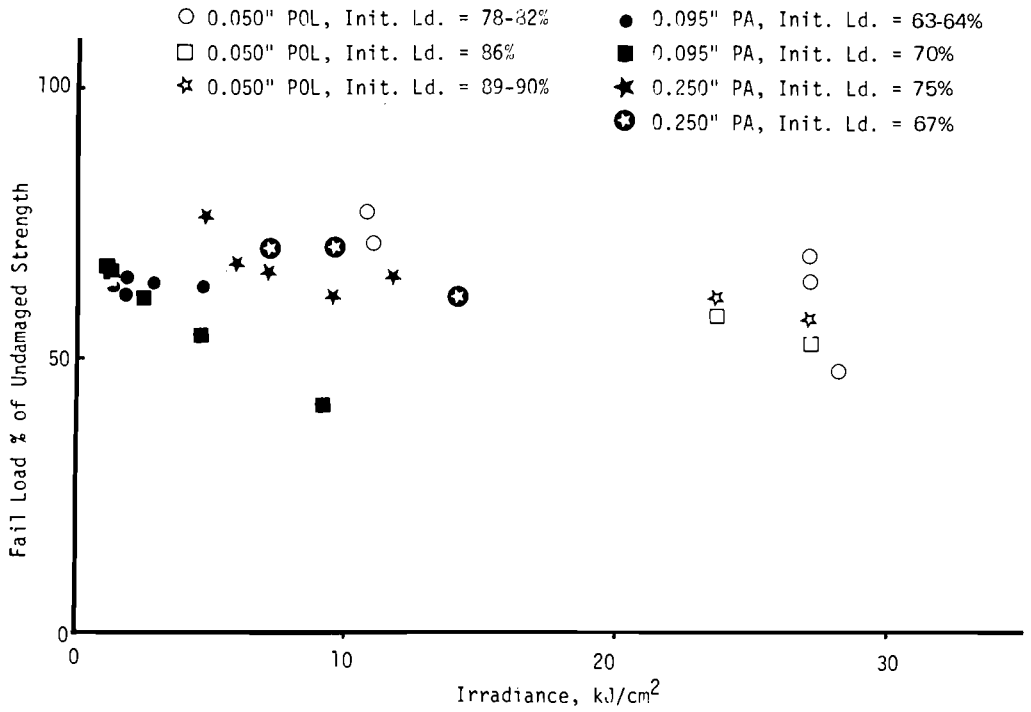

Figure 12. Fail strength versus irradiance at various initial load (≠ 0) levels - 0.050", 0.095", and 0.250" plates.

during the laser heating shows that at the higher irradiances the initial load drops off to a much lower minimum level than at the lower irradiances. The explanation could lie in the laser-on-time differences for high and low irradiance and the different load-time experiences of the specimens. The data of Figure 14 for the thicker plates shows a general increase in failure strength with increasing initial load for all levels of irradiance. (Again there is a large gap in data.) The explanation of this phenomenon will require further examination of the load time histories of the specimens, analysis of the relative stiffnesses of tension plate and tension test machine, and the generation of data for initial loads between 0% and 65%.

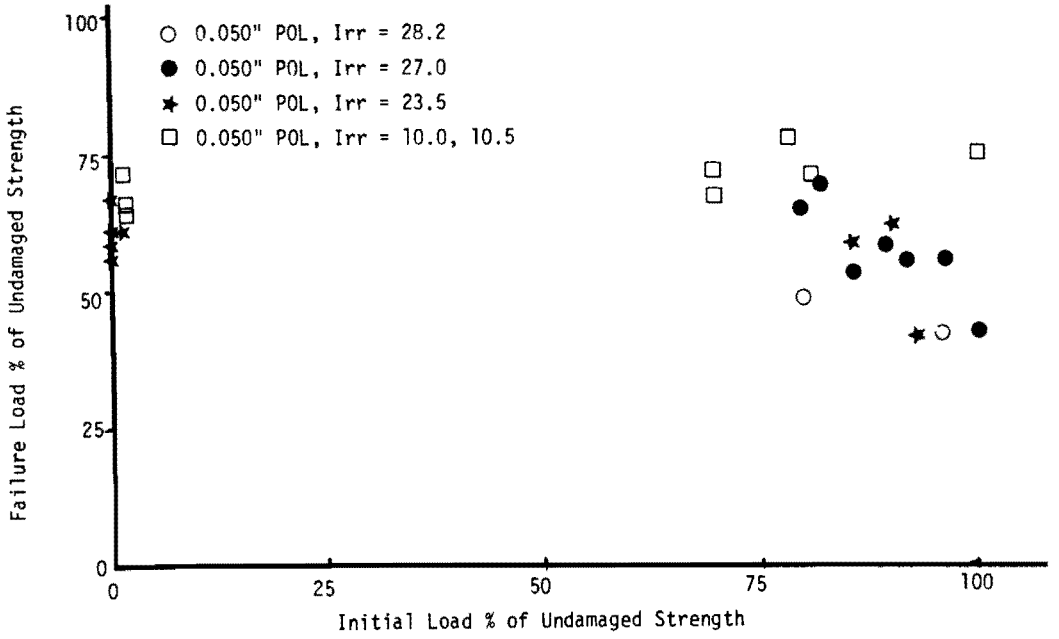

Figure 13. Failure load versus initial load at various irradiance levels - 0.050" POL plates.

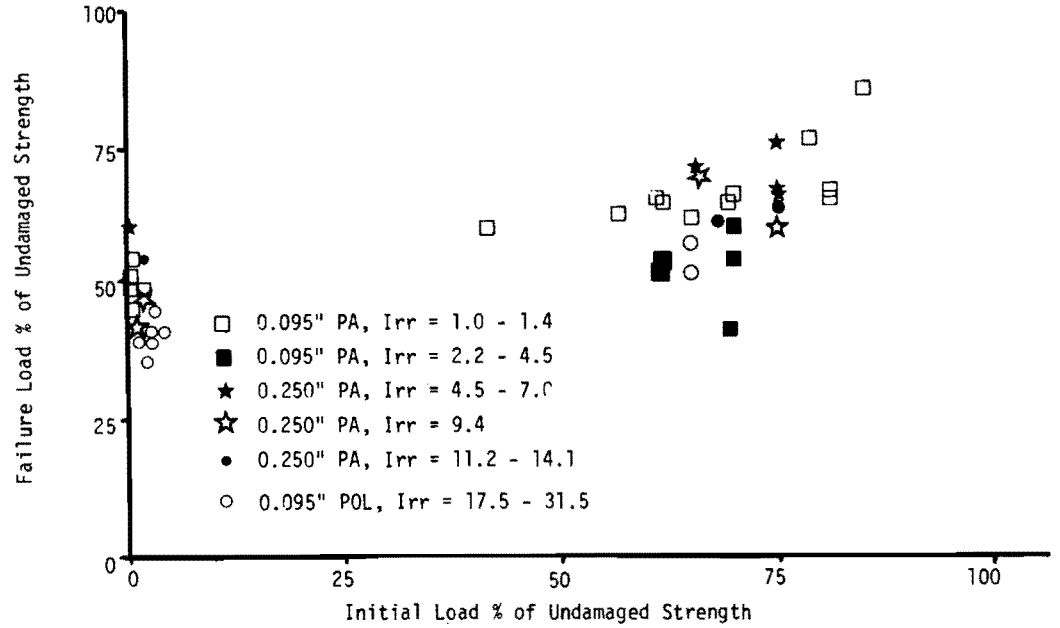

Figure 14. Failure load versus initial load at various irradiance levels - 0.095" PA and 0.250" PA plates.

Fracture Mechanics Considerations. Table 3 provides computed K_c fracture toughness (or stress intensity factors) for all the plate tests assuming the damaged plates to be represented by a central-through-cracked plate. Four of the 0.250"-thick plates do not fit this model since only a portion of the thickness of each was affected by the laser. Although the correction factor to through-crack values to account for a surface crack may be small for the four plates in question, the obvious disparity from the through-crack assumptions requires the disregard of these data values until further examination is made. This subject is covered extensively by Brown and Srawley.[4] The data in Table 3 has been further reduced to provide the analysis shown in Table 4. Comparison of the magnitudes of the tabulated K_c values for zero-initial-load COLD tests to the values of undamaged material (42.0, 41.4, and 36.5 ksi$\sqrt{\text{in.}}$ for 0.050", 0.100", and 0.250" thick plates, respectively) indicates that the material controlling the fracture strength of the plate has not changed drastically. The HOT and DELAY tests show significantly higher effective toughness which is probably attributable to the higher temperature at which failure occurred in these tests.

The most significant effect is shown by the difference between initial load = 0 and initial load = 0. A significant increase in failure strength is attributable to the initial load during laser damage. The probable explanation for this is that the initial load results in a residual compression in the material which increases the apparent stress at which failure occurs.

Another significant effect evident in Table 4 is in the relative strengths demonstrated by HOT, DELAY, and COLD tests. HOT strengths are consistently greater than DELAY strengths and COLD strengths. DELAY strengths are either equivalent to or greater than COLD strengths. COLD strengths are the lowest. COLD strength with no initial load during laser damage is less than COLD strength with initial load. Therefore, the worst sequence of events is to have laser damage take place without applied load and the load to be applied after laser heating has dissipated.

The question of scatter in data and the need for statistical analysis is addressed by Figure 15. Although the general trends of increased K_c with increased initial load apparent in this figure, the existence of a large amount of scatter is also quite evident. The need for further study is indicated to reduce the scatter or accommodate the scatter in survivability analyses by application of statistical concepts and procedures.

Analysis of Test Results for Torsion Tubes

Limitations on Failure Modes. Compared to the tension plate data the torsion tube data is very sparse at this time. The most serious lack is the absence of tube behavior data for laser irradiation covering a larger length along the axis of the tube equal to about 1.5 x the diameter. Under this type of extended radiation degradation of material properties could precipitate failure of general instability mode at lower loads or at lower levels of material degradation than the yielding local crippling type of failure experienced in the present test series.

4. BROWN, W. F., Jr., and SRAWLEY, J. E. *Plane Strain Crack Toughness Testing of High Strength Metallic Materials.* ASTM STP 410, 1969.

Table 3. CALCULATED K_c VALUES FOR TENSION PLATES

Test No.	L_2[1] (in.)	TLD[2] (in.)	Fail σ Type[3] (ksi)	K_c[5] L_2 (ksi√in.)	K_c[5] TLD (ksi√in.)	Init. Load (%[4])	Irr (kJ/cm²)
			a. 0.050" Thickness				
1943	0.3	0.05	57.7C	39.5	16.2	0	10.5
1944	0.4	0.05	54.3C	43.0	15.3	0	10.5
1945	0.4	0.2	52.0C	41.2	29.0	0	10.5
1946	0.8	0.65	43.4C	49.9	44.5	0	0.77*
1951	0.3	0.45	62.3C	42.7	52.5	0	7.0
1952	0.25	0.10	57.7C	36.0	22.8	0	7.0
1953	0.4	0.30	54.3C	43.0	37.2	0	7.0
1957	0.2	0.1	64.6C	36.0	25.6	0	7.0
2066	0.5	0.45	57.7C	51.4	48.6	69	10.5
2067	0.35	0.45	62.9C	46.5	53.0	78	10.5
2068	0.55	0.6	58.3C	54.6	57.2	81	10.5
2072	0.6	0.45	54.9C	53.9	46.2	69	10.5
5012	0.8	( )	45.7C	52.6	( )	0	29.2†
5013	0.5	0.15	50.3C	44.8	24.3	0	27.0†
5014	0.3	( )	56.6C	38.8	( )	0	18.0†
5015	0.7	0.3	60.0C	64.1	41.1	0	18.0†
5016	0.3	( )	58.9C	40.3	( )	0	18.0†
5032	0.7	0.7	52.0C	55.6	55.6	79	27.0†
5033	0.6	0.6	56.0C	55.0	55.0	82	27.0
5034	0.9	0.7	42.9C	53.0	45.8	86	27.0
5035	0.9	0.75	46.3C	57.2	51.4	89	27.0
5036	0.8	0.63	45.1C	51.9	45.4	93	27.0
5037	0.9	0.8	44.6C	55.1	51.3	96	27.0
5038	0.8	( )	34.3D	39.5	( )	100	27.0
5057	0.6	0.3	45.7C	44.9	31.3	0	23.5
5058	0.6	0.4	46.9C	46.0	37.2	0	23.5
5059	0.7	0.45	44.6C	47.7	37.6	0	23.5
5066	0.9	1.02	39.4C	48.7	52.5	79	28.2
5075	0.5	0.55	59.4H	52.9	55.6	100	10.0
5076	0.9	1.0	42.9D	53.0	56.5	97	26.0
5077	0.75	0.85	34.3D	38.1	41.0	97	28.2
5078	0.9	1.0	33.1D	40.9	43.6	93	23.5
5079	0.85	1.0	30.9D	36.9	40.7	93	21.0
5080	0.7	0.8	47.4C	50.6	54.6	86	23.5
5082	0.7	0.8	49.7D	53.1	57.2	90	23.5
5083	0.5	( )	48.0C	42.7	( )	0	23.5
5084	0.5	0.34	48.0C	42.7	35.0	0	23.5
5085	0.7	0.20	54.3C	58.0	30.3	0	23.5
			b. 0.095" Thickness				
1941	0.7	0.45	33.4C	37.0	28.1	0	1.47
1948	0.55	0.5	42.4C	39.7	37.8	0	1.05
1949	0.55	0.5	40.0C	37.4	35.6	0	1.05
1950	0.5	0.5	44.2C	39.4	35.1	0	1.05
1954	0.5	0.4	43.3C	38.5	34.3	0	0.70
1955	0.5	0.35	44.2C	39.4	32.7	0	0.70
1956	0.5	0.35	45.1C	40.2	33.4	0	0.70
2070	0.55	0.6	55.6C	52.0	54.6	64	1.05
2071	0.55	0.65	54.4C	50.9	55.7	64	1.40
2073	0.6	0.85	45.4C	44.6	54.2	64	17.5†
2074	0.45	0.65	50.8C	42.8	52.1	64	17.5†
5017	0.65	0.63	30.7C	31.5	31.0	0	31.5†
5018	0.55	0.55	33.7C	31.5	31.5	0	31.5†
5019	0.5	0.5	35.5C	31.6	31.6	0	31.5†
5020	0.55	0.5	34.3C	32.1	30.5	0	24.7†
5021	0.5	0.5	36.1C	32.1	32.1	0	20.2†
5022	0.35	0.4	38.5C	28.5	30.5	0	20.2†
5039	0.9	1.1	36.1D	44.6	50.6	70	9.0
5040	0.7	0.85	46.9D	50.0	56.0	70	4.5
5041	0.6	0.7	53.5D	52.5	57.2	70	2.2
5042	0.5	0.55	57.7D	51.4	54.0	70	1.1
5043	0.55	0.5	52.6C	49.2	46.8	43	1.1
5044	0.55	0.55	55.3C	51.8	51.8	57	1.1
5045	0.6	0.5	57.1C	56.0	50.8	63	1.1
5046	0.8	0.9	46.9D	54.0	57.9	63	4.5
5047	0.6	0.7	54.1D	53.1	57.9	63	2.7
5067	0.5	0.55	56.8C	50.6	53.2	70	1.2
5068	0.5	0.4	75.1H	66.9	59.5	86	1.2
5069	0.5	0.5	58.6D	52.2	52.2	78	1.2
5070	0.55	0.65	57.1D	53.4	58.5	81	1.2
5071	0.55	0.6	58.6D	54.8	57.5	81	1.2
5072	0.55	0.45	46.9C	43.9	39.5	0	1.2
5073	0.55	0.5	45.1C	42.2	40.2	0	1.2
5074	0.5	0.5	42.4C	37.8	37.8	0	1.2
			c. 0.250" Thickness				
5026	0.55	( )	67.4C	63.1**	( )	0	2.25
5027	0.55	( )	69.7C	65.2**	( )	0	3.15
5028	0.55	0.6	51.8C	48.5**	50.8	0	4.50
5029	1.1	0.95	28.8C	40.4	36.6	0	22.8
5030	0.7	( )	46.3C	49.5	( )	0	11.2
5090	0.8	1.0	56.0H	64.5	73.6	75	11.7
5091	0.6	0.7	52.1D	51.1	55.7	75	9.4
5092	0.55	0.7	65.8C	61.6**	70.3	75	4.7
5093	0.6	0.8	57.1D	56.0	65.7	75	7.0
5094	0.6	0.8	57.7D	56.6	66.4	75	5.9
5095	0.6	0.5	60.2C	59.1	53.8	67	7.0
5096	0.7	0.8	60.6C	64.8	69.8	67	9.4
5097	0.8	1.2	53.3D	61.4	79.4	67	14.1
5098	0.65	( )	40.5C	41.5	( )	0	9.4
5099	0.65	( )	35.2C	36.1	( )	0	9.4
5100	0.75	0.6	37.0C	41.1	36.3	0	9.4

*Painted

†Polished surface. All 0.095" thick plates were painted except as noted. All 0.250" thick plates were painted.

‡Natural surface. All 0.050" thick plates were polished except as noted.

**Melt zone did not penetrate thickness. Through-crack equations do not hold.

Notes:
1. Width of melt zone.
2. Width of actual crack or hole.
3. C = COLD, D = DELAY, H = HOT.
4. % = Percent of undamaged strength.
5. K_c based on center through-cracked sheet.

$K_c = \sigma\sqrt{a}\, f(\lambda)$

$\sigma = P/A$ A = Cross section area

2a = "crack" length = L_2 or TLD

$f(\lambda) = 1.77[1 - 0.1\lambda + \lambda^2]$

$\lambda = 2a/W$, W = plate width

Table 4. AVERAGE K_c VALUES, 7075-T6 Al TENSION PLATES

Test Conditions	$\bar{K}_c$ (ksi√in.) Plate Thickness (in.) 0.050	0.095	0.250
A. All Tests	[42.0]	[41.4]	[36.5]
1. Crack Length = L_2	47.4	43.5	53.8
2. Crack Length = TLD	36.6	44.0	41.1
3. Crack Length = Largest of L_2 and TLD	48.6	46.5	58.0
a. Initial Load = 0	45.5(19)	36.6(16)	48.5(8)
b. Initial Load ≠ 0	51.8(19)	55.3(18)	67.5(8)
B. Selected Tests (Using Crack Length = Larger of L_2 and TLD)			
1. HOT Tests	55.6(1)	66.9(1)	73.6(1)
2. DELAY Tests	46.4(6)	55.8(9)	66.8(4)
3. COLD Tests	48.8(31)	42.1(24)	53.3(11)
a. Initial Load = 0	45.5(19)	36.6(16)	48.5(8)
b. Initial Load ≠ 0	54.2(12)	53.4(8)	64.6(3)

Notes: Calculated for center cracked plate.
Numbers in ( ) are number of tests.
Values in [ ] are K_c values for undamaged material at room temperature.

The failures reported here were all of the HOT type. COLD tests have not been performed as yet on the unfailed tubes. Instrumentation for measuring time-coordinated temperatures and strain had not been completed in time for the present test series so DELAY test type data was not recorded.

Failure of Laser Irradiated Tubes. Based on the data of Table 2 the combinations of irradiance and initial load required to cause failure of rotating tubes, 0.050" thick, are shown in Figure 16. With zero initial load average irradiation levels of less than 10 kJ/cm^2 in the Ford laser beam produced complete burnthrough of painted tubes. With the AFML laser, cracking of painted tubes tantamount to failure developed at average irradiances of less than 12 kJ/cm^2 in the laser beam. With application of initial load during irradiation of 9% and 18% of undamaged strength, failure occurred at average irradiance levels of less than 5 kJ/cm^2 in the beam. Additional data are listed in Table 2.

The failure modes under load (some of which can be seen in Figure 6) occurred with little, if any, evidence of severe material degradation. Yielding or crippling failure to occur at 9% or 18% of undamaged strength requires the degradation of the material strength to 9% to 18% of undamaged material strength. This apparently is easily done. A lesser degradation of material strength over a large enough area to cause general instability should be easily accomplished with a laser of slightly higher power.

Examination of the data in Table 2b and 2c indicates that to produce damage sufficient for failure in 0.095"-thick tubes required 4 to 5 times the average beam irradiance required for similar damage in the 0.050"-thick tubes when the AFML laser was used. The TSL MICOM tests showed the need for only twice the irradiance for 0.095" tubes as for 0.050" tubes and 2-1/2 to 4 times the 0.050" tube requirement for 0.250" thick tubes. The differences in beam quality of the TSL MICOM and AFML lasers, especially in the power density distributions, are major and significant differences in their effects could be expected. As discussed earlier these differences tend to preclude comparison between lasers.

The Ford laser was not able to produce failure in the 0.095" tubes although the peak irradiances received by the specimen were higher than attained in the AFML tests. However, to attain the high irradiance required reduction of the laser beam to 0.3" and 0.2" diameter compared to the 0.6" diameter maintained at AFML. The smaller size undoubtedly reduced the heat buildup and temperature increase through the 0.095" thickness.

SUMMARY AND CONCLUSIONS

The major observations can be summarized as follows. (1) Well-defined qualitative correlations between physical damage descriptors L_2 or TLD and laser irradiances on painted plate specimens indicate that reliable quantitative relationships can be found. Similarly reliable relationships for polished specimens are unlikely. (2) The force of gravity acting on the flow of melted metal affects

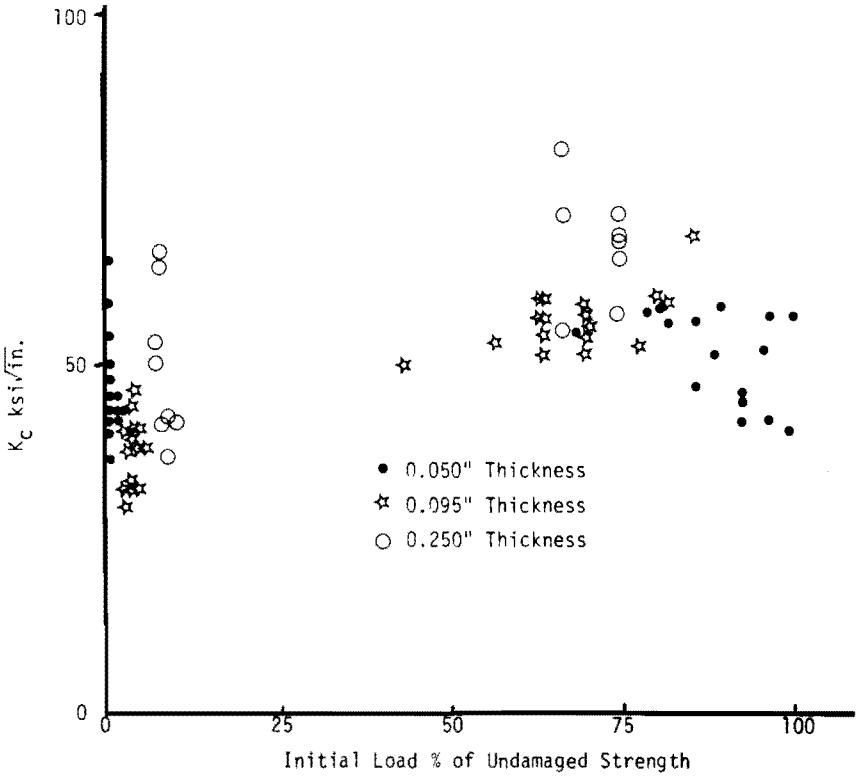

Figure 15. K_c versus initial load during damage, 7075-T6 Al plates.

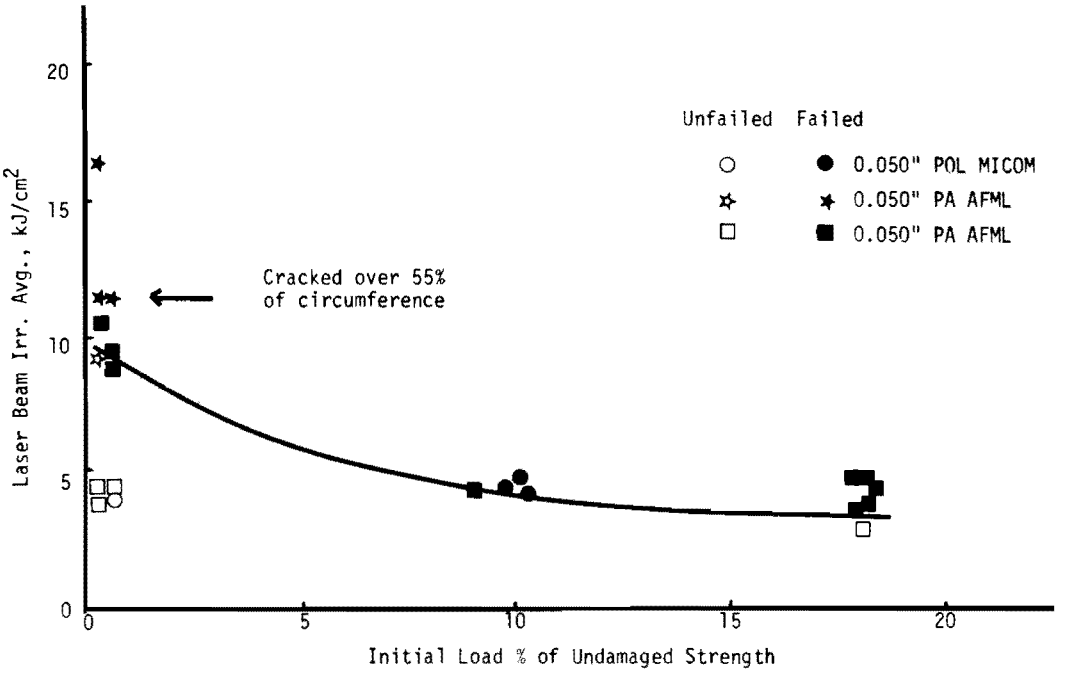

Figure 16. Irradiance for failure of rotating tubes for various initial loads - 0.050" thick tubes.

the resulting damage in tension plates and can affect the residual strength depending on the orientation of the direction of major load relative to the gravitational direction. (3) Increased irradiance results in reduced failure strength for constant or zero initial load values. (4) Initial load effects on failure strength are mixed. Increasing initial load above 65% causes a downward trend in failure strength in thinner plates (0.050") and an upward trend in failure strength in thicker plates (0.095" and 0.250"). Further investigation of various thicknesses of tension plates with emphasis on load-time history under combined load and laser irradiation and on the effect of the relative stiffness of tension plate to testing machine stiffness is necessary. Data for initial load values between 0% and 65% of undamaged strength are required. (5) Based on comparison of average computed K_c values the application of initial load during laser damage produces higher failure strength compared to zero-initial-load failure strength. Therefore initial load is beneficial. (6) Based on comparison of averaged computed K_c values COLD strength is generally significantly lower than HOT and DELAY failure strength.

DISTRIBUTION LIST

No. of Copies	To
1	Office of the Director, Defense Research and Engineering, The Pentagon, Washington, D.C. 20301
12	Commander, Defense Documentation Center, Cameron Station, Building 5, 5010 Duke Street, Alexandria, Virginia 22314
1	Metals and Ceramics Information Center, Battelle Columbus Laboratories, 505 King Avenue, Columbus, Ohio 43201
	Deputy Chief of Staff, Research, Development, and Acquisition, Headquarters Department of the Army, Washington, D. C. 20310
1	ATTN: DAMA-ARZ
	Commander, Army Research Office, P. O. Box 12211, Research Triangle Park, North Carolina 27709
1	ATTN: Information Processing Office
1	Dr. F. W. Schmiedeshoff
	Commander, U. S. Army Materiel Development and Readiness Command, 5001 Eisenhower Avenue, Alexandria, Virginia 22333
1	ATTN: DRCLDC, Mr. R. Zentner
	Commander, U. S. Army Communications Research and Development Command, Fort Monmouth, New Jersey 07703
1	ATTN: DRCDO-GG-TD
1	DRCDO-GG-OM
1	DRCDO-GG-E
1	DRCDO-GG-EA
1	DRCDO-GG-ES
1	DRCDO-GG-EG
1	DRCDO-GG-EI
	Commander, U. S. Army Missile Research and Development Command, Redstone Arsenal, Alabama 35809
1	ATTN: DRDMI-RKK, Mr. C. Martens, Bldg. 7120
	Commander, U. S. Army Natick Research and Development Command, Natick, Massachusetts 01760
1	ATTN: Technical Library
1	Dr. E. W. Ross
1	DRDNA-UE, Dr. L. A. McClaine
	Commander, U. S. Army Satellite Communications Agency, Fort Monmouth, New Jersey 07703
1	ATTN: Technical Document Center
	Commander, U. S. Army Tank-Automotive Research and Development Command, Warren, Michigan 48090
1	ATTN: DRDTA-RKA
1	DRDTA-UL, Technical Library
	Commander, U. S. Army Armament Research and Development Command, Dover, New Jersey 07801
2	ATTN: Technical Library
1	DRDAR-SCM, J. D. Corrie
1	Dr. J. Fraiser
	Commander, White Sands Missile Range, New Mexico 88002
1	ATTN: STEWS-WS-VT
	Commander, Aberdeen Proving Ground, Maryland 21005
1	ATTN: STEAP-TL, Bldg. 305
	Commander, U. S. Army Armament Research and Development Command, Aberdeen Proving Ground, Maryland 21010
1	ATTN: DRDAR-QAC-E
	Commander, U. S. Army Ballistic Research Laboratory, Aberdeen Proving Ground, Maryland 21005
1	ATTN: Dr. R. Vitali
1	Dr. W. Gillich
1	Mr. A. Elder
	Commander, Harry Diamond Laboratories, 2800 Powder Mill Road, Adelphi, Maryland 20783
1	ATTN: Technical Information Office
	Commander, Picatinny Arsenal, Dover, New Jersey 07801
1	ATTN: Mr. A. M. Anzalone, Bldg. 3401
1	Mr. J. Pearson
1	G. Randers-Pehrson
1	SARPA-RT-S
	Commander, Redstone Scientific Information Center, U. S. Army Missile Research and Development Command, Redstone Arsenal, Alabama 35809
1	ATTN: DRDMI-TB
	Commander, Watervliet Arsenal, Watervliet, New York 12189
1	ATTN: Mr. D. P. Kendall
1	Mr. J. F. Throop
	Commander, U. S. Army Foreign Science and Technology Center, 220 7th Street, N. E., Charlottesville, Virginia 22901
1	ATTN: Mr. Marley, Military Tech
	Chief, Benet Weapons Laboratory, LCWSL, USA ARRADCOM, Watervliet Arsenal, Watervliet, New York 12189
1	ATTN: DRDAR-LCB-TL
	Director, Eustis Directorate, U. S. Army Air Mobility Research and Development Laboratory, Fort Eustis, Virginia 23604
1	ATTN: Mr. J. Robinson, DAVDL-E-MOS (AVRADCOM)
	U. S. Army Aviation Training Library, Fort Rucker, Alabama 36360
1	ATTN: Building 5906-5907
	Commander, U. S. Army Agency for Aviation Safety, Fort Rucker, Alabama 36362
1	ATTN: Librarian, Bldg. 4905
	Commander, USACDC Air Defense Agency, Fort Bliss, Texas 79916
1	ATTN: Technical Library
	Commander, U. S. Army Engineer School, Fort Belvoir, Virginia 22060
1	ATTN: Library
	Commander, U. S. Army Engineer Waterways Experiment Station, Vicksburg, Mississippi 39180
1	ATTN: Research Center Library
	Commander, Naval Air Engineering Center, Lakehurst, New Jersey 08733
1	ATTN: Technical Library, Code 1115
	Director, Structural Mechanics Research, Office of Naval Research, 800 North Quincy Street, Arlington, Virginia 22203
1	ATTN: Dr. N. Perrone
	Naval Air Development Center, Aero Materials Department, Warminster, Pennsylvania 18974
1	ATTN: J. Viglione
	David Taylor Naval Ship Research and Development Laboratory, Annapolis, Maryland 21402
1	ATTN: Dr. H. P. Chu
	Naval Research Laboratory, Washington, D.C. 20375
1	ATTN: C. D. Beachem, Head, Adv. Mat'ls Tech Br. (Code 6310)
1	Dr. J. M. Krafft - Code 8430
	Chief of Naval Research, Arlington, Virginia 22217
1	ATTN: Code 471
	Naval Weapons Laboratory, Washington, D.C. 20390
1	ATTN: H. W. Romine, Mail Stop 103
1	Ship Research Committee, Maritime Transportation Research Board, National Research Council, 2101 Constitution Avenue, N. W., Washington, D.C. 20418
	Air Force Materials Laboratory, Wright-Patterson Air Force Base, Ohio 45433
2	ATTN: AFML (MXE), E. Morrissey
1	AFML (LC)
1	AFML (LLP), D. M. Forney, Jr.
1	AFML (MBC), Mr. Stanley Schulman
	Air Force Flight Dynamics Laboratory, Wright-Patterson Air Force Base, Ohio 45433
1	ATTN: AFFDL (FBS), C. Wallace
1	AFFDL (FBE), G. D. Sendeckyj

No. of Copies	To
	National Aeronautics and Space Administration, Washington, D.C. 20546
1	ATTN: Mr. B. G. Achhammer
1	Mr. G. C. Deutsch - Code RW
	National Aeronautics and Space Administration, Marshall Space Flight Center, Huntsville, Alabama 35812
1	ATTN: R. J. Schwinghamer, EH01, Dir., M&P Lab
1	Mr. W. A. Wilson, EH41, Bldg. 4612
	National Aeronautics and Space Administration, Langley Research Center, Hampton, Virginia 23665
1	ATTN: Mr. H. F. Hardrath, Mail Stop 188M
1	Mr. R. Foye, Mail Stop 188A
1	Dr. R. J. Hayduk, Mail Stop 243
	National Aeronautics and Space Administration, Lewis Research Center, 21000 Brookpark Road, Cleveland, Ohio 44135
1	ATTN: Mr. S. S. Manson
1	Mr. R. F. Lark, Mail Stop 49-3
	Section,
	Lockheed-Georgia Company, 86 South Cobb Drive, Marietta, Georgia 30063
1	ATTN: Materials & Processes Eng. Dept. 71-11, Zone 54
	National Bureau of Standards, U. S. Department of Commerce, Washington, D.C. 20234
1	ATTN: Mr. J. A. Bennett
1	Mechanical Properties Data Center, Belfour Stulen Inc., 13917 W. Bay Shore Drive, Traverse City, Michigan 49684
	Midwest Research Institute, 425 Coker Boulevard, Kansas City, Missouri 64110
1	ATTN: Mr. C. Q. Bowles
1	Dr. J. Charles Grosskreutz, Asst. Dir. for Research, Solar Energy Research Institute, 1536 Cole Boulevard, Golden, Colorado 80401
1	Mr. A. Hurlich, Convair Div., General Dynamics Corp., Mail Zone 630-01, P. O. Box 80847, San Diego, California 92138
	Southwest Research Institute, 8500 Culebra Road, San Antonio, Texas 78284
1	ATTN: Dr. P. Francis
1	Dr. W. Baker
1	Dr. E. A. Steigerwald, TRW Metals Division, P. O. Box 250, Minerva, Ohio 44657
1	Dr. George R. Irwin, Department of Mechanical Engineering, University of Maryland, College Park, Maryland 20742
	Battelle Columbus Laboratories, 505 King Avenue, Columbus, Ohio 43201
1	ATTN: Mr. J. Campbell
	General Electric Company, Schenectady, New York 12309
1	ATTN: Mr. H. F. Bueckner, Large Steam Turbine Generator Department
	General Electric Company, Knolls Atomic Power Laboratory, P. O. Box 1072, Schenectady, New York 12301
1	ATTN: Mr. F. J. Mehringer
1	Dr. L. F. Coffin, Room 1C41-K1, Corp. R&D, General Electric Company, P. O. Box 8, Schenectady, New York 12301
	United States Steel Corporation, Monroeville, Pennsylvania 15146
1	ATTN: Dr. A. K. Shoemaker, Research Laboratory, Mail Stop 78
	Westinghouse Electric Company, Bettis Atomic Power Laboratory, P. O. Box 109, West Mifflin, Pennsylvania 15122
1	ATTN: Mr. M. L. Parrish
	Westinghouse Research and Development Center, 1310 Beulah Road, Pittsburgh, Pennsylvania 15235
1	ATTN: Mr. E. T. Wessel
1	Mr. M. J. Manjoine
1	Dr. Alan S. Tetelman, Failure Analysis Associates, Suite 4, 11777 Mississippi Ave., Los Angeles, California 90025
	Brown University, Providence, Rhode Island 02912
1	ATTN: Prof. W. N. Findley, Division of Engineering, Box D
	Carnegie-Mellon University, Department of Mechanical Engineering, Schenley Park, Pittsburgh, Pennsylvania 15213
1	ATTN: Dr. J. L. Swedlow
1	Prof. J. D. Lubahn, Colorado School of Mines, Golden, Colorado 80401
1	Prof. J. Dvorak, Civil Engineering Department, Duke University, Durham, North Carolina 27706
	George Washington University, School of Engineering and Applied Sciences, Washington, D.C. 20052
1	ATTN: Dr. H. Liebowitz
	Terra Tek, University Research Park, 420 Wakara Way, Salt Lake City, Utah 84108
1	ATTN: Dr. A. Jones
	P. R. Mallory Company, Inc., 3029 East Washington Street, Indianapolis, Indiana 46206
1	ATTN: Technical Library
1	Librarian, Material Sciences Corporation, Blue Bell Office Campus, Merion Towle House, Blue Bell, Pennsylvania 19422
	Massachusetts Institute of Technology, Cambridge, Massachusetts 02139
1	ATTN: Prof. F. A. McClintock, Room 1-304
1	Prof. T. H. H. Pian, Department of Aeronautics and Astronautics
1	Prof. A. S. Argon, Room 1-3D6
1	Prof. J. N. Rossettos, Department of Mechanical Engineering, Northeastern University, Boston Massachusetts 02115
1	Prof. R. Greif, Department of Mechanical Engineering, Tufts University, Medford, Massachusetts 02155
1	Dr. D. E. Johnson, AVCO Systems Division, Wilmington, Massachusetts 01887
	University of Delaware, Department of Aerospace and Mechanical Engineering, Newark, Delaware 19711
1	ATTN: Prof. B. Pipes
1	Prof. J. Vinson
	Syracuse University, Department of Chemical Engineering and Metallurgy, 409 Link Hall, Syracuse, New York 13210
1	ATTN: Mr. H. W. Liu
1	Prof. W. Goldsmith, Department of Mechanical Engineering, University of California, Berkeley, California 94720
1	Prof. A. J. McEvily, Metallurgy Department U-136, University of Connecticut, Storrs, Connecticut 06268
1	Prof. D. Drucker, Dean of School of Engineering, University of Illinois, Champaign, Illinois 61820
	University of Illinois, Urbana, Illinois 61801
1	Dr. T. Lardner, Department of Theoretical and Applied Mechanics
1	Prof. R. I. Stephens, Materials Engineering Division, University of Iowa, Iowa City, Iowa 52242
1	Prof. D. K. Felbeck, Department of Mechanical Engineering, University of Michigan, 2046 East Engineering, Ann Arbor, Michigan 48109
1	Dr. M. L. Williams, Dean of Engineering, 240 Benedum Hall, University of Pittsburgh, Pittsburgh, Pennsylvania 15260
1	Prof. A. Kobayashi, Department of Mechanical Engineering, FU-10, University of Washington, Seattle, Washington 98195
	State University of New York at Stony Brook, Stony Brook, New York 11790
1	ATTN: Prof. Fu-Pen Chiang, Department of Mechanics
	Denver Research Institute, 2390 South University Boulevard, Denver, Colorado 80210
1	ATTN: Dr. R. Recht
	Director, Army Materials and Mechanics Research Center, Watertown, Massachusetts 02172
2	ATTN: DRXMR-PL
1	DRXMR-AG-MD